Published OnlineFirst May 21, 2012; DOI:10.1158/2159-8290.CD-12-0009

The response rate for crizotinib in patients with *ALK*-rearranged NSCLCs in the trial was shown to be 57%, with a disease control rate of up to 90% (32). Furthermore, the median overall survival for crizotinib treatment was not determinable within the follow-up period of 18 months (40). Comparison of crizotinib treatment with a historical control was further striking. Whereas the median overall survival was not achieved for patients who received crizotinib as a second- or third-line treatment, it was only 6 months for the *ALK*-rearranged control patients who received conventional chemotherapy in the second- or third-line setting.

While crizotinib can inhibit MET kinase activity and *MET* may become amplified in NSCLCs (41), there was no *MET* amplification present in the above *EML4-ALK*-positive cohort (32). Similarly, while ROS1 tyrosine kinase is sensitive to crizotinib (42), a recent large-scale screening of gene fusions among NSCLC ($n = 1,529$) revealed a complete mutual exclusiveness between *ALK* and *ROS1* fusions (43). Furthermore, the mechanism for the insensitivity of *ALK* fusion-positive tumors to crizotinib has been mostly secondary mutations within the kinase domain of EML4-ALK (see below). These data evidence that crizotinib exerts its marked therapeutic efficacy in NSCLCs through specific suppression of EML4-ALK activity.

These observations clearly supported the clinical use of ALK inhibitors for the treatment of *EML4-ALK*-positive NSCLC. Indeed, on August 26, 2011, the U.S. Food and Drug Administration approved crizotinib as a treatment for *ALK*-rearranged NSCLCs. From the time of our first report of the identification of *EML4-ALK* in 2007, it took only 4 years for the first ALK inhibitor to be approved for use in the clinic, which is a record for cancer drug development (44).

OTHER *ALK* TRANSLOCATIONS IN EPITHELIAL TUMORS

Following the discovery of *EML4-ALK*, efforts have expanded to detect novel ALK fusions in epithelial tumors. Development of a sensitive immunohistochemical technique (intercalated antibody-enhanced polymer method, or iAEP) to stain ALK proteins in FFPE specimens led to the identification of several NSCLC samples that were positive with this approach but negative for *EML4-ALK* with multiplex RT-PCR (34). Further investigation of these specimens revealed the presence of another fusion of *ALK*, *KIF5B-ALK*. Similar to EML4-ALK, KIF5B contains dimerization motifs that play an essential role in the oncogenic activity of KIF5B-ALK and there are now known to be several variants of KIF5B-ALK (45). Togashi and colleagues reported still another *ALK* fusion, *KLC1-ALK*, in NSCLCs (46).

Yet another novel *ALK* fusion, *VCL-ALK*, was recently identified in a tumor of unclassified renal cell carcinoma with renal medullary carcinoma (RMC) characteristics that developed in a 16-year-old boy with sickle cell trait (47). VCL-ALK was also detected in RMCs isolated from a 6-year-old boy (48). RMC mostly affects young individuals and has a poor outcome, but the discovery of *VCL-ALK* has raised the possibility of effective treatment with an ALK inhibitor for patients who harbor this fusion gene. Furthermore, screening of tissue microarrays of renal cell carcinoma with the iAEP technique led to the detection of single cases each positive for *TPM3-ALK* or *EML4-ALK* (E2;A20 variant; ref. 16).

ONCOGENIC POINT MUTATIONS IN ALK

Neuroblastoma

Attempts by several groups to identify genes underlying neuroblastoma through different approaches (mapping of single-nucleotide polymorphisms for familial neuroblastoma and chromosome copy number analysis for sporadic neuroblastoma) resulted in the almost simultaneous identification of activating mutations within *ALK* (Figs. 2 and 3; refs. 18–21). About 10% of sporadic neuroblastoma cases harbor somatic nonsynonymous mutations within ALK, including K1062M, F1174L/C/I, F1245C/V/L, and R1275Q amino acid substitutions. On the other hand, a distinct but partially overlapping set of ALK mutations (T1087I, G1128A, R1275Q, and others) has been identified in familial neuroblastoma.

Importantly, these mutations do not confer equal transforming ability. The F1174L mutant, for instance, efficiently phosphorylates the signaling molecules STAT3 and AKT, but not extracellular signal-regulated kinase (ERK)1/2, whereas the R1275Q mutant efficiently phosphorylates ERK1/2 but not STAT3 (18). Knockdown experiments revealed that the growth of neuroblastoma cell lines was dependent to a greater extent on the F1174L mutant than on R1275Q (18, 20). The mutant ALK proteins thus contribute substantially to the transformation process in neuroblastoma, but the extent to which they do so varies among the mutation types.

These mutations also differentially affect the sensitivity of neuroblastoma to ALK inhibitors (49, 50), which may not be surprising given that point mutations within the kinase domain of ALK affect its 3-dimensional structure (including that of the inhibitor binding cleft) and thereby influence inhibitor binding. The F1174L mutant confers marked resistance to crizotinib in a cell-based assay (49, 50), suggesting that this amino acid substitution not only increases the enzymatic activity of ALK by changing the structure of the kinase domain but by doing so also affects the binding of ALK inhibitors.

The I1250T mutation of ALK was recently identified in an individual with neuroblastoma and was shown to abolish the activity of the enzyme (51). Each ALK mutation identified in neuroblastoma therefore needs to be assessed for how (or if) it contributes to carcinogenesis.

Anaplastic Thyroid Cancer

Nucleotide sequencing of *ALK* exons encoding the kinase domain in cell lines and fresh specimens of thyroid cancer (52) revealed novel missense mutations specifically in anaplastic thyroid cancer (ATC) samples (2 positive samples of 11). Each of the 2 identified amino acid substitutions (L1198F and G1201E) increased the enzymatic activity of ALK and induced the formation of transformed foci when introduced into mouse 3T3 cells, clearly indicating the activating nature of these mutations. It is thus likely that a subset of ATC and neuroblastoma cases share the same transforming gene, but it remains to be determined whether the *ALK* mutation profiles differ between the 2 disorders.

Published OnlineFirst May 21, 2012; DOI:10.1158/2159-8290.CD-12-0009

GENE AMPLIFICATION OF *ALK*

In addition to nonsynonymous mutations, *ALK* infrequently becomes amplified in neuroblastoma (21, 53). While its clinical relevance is yet to be clarified, *ALK* amplification frequently co-occurs with amplification of *MYCN* amplification, a known growth driver for this disorder, suggesting that *ALK* also contributes to carcinogenesis.

Recently, van Gaal and colleagues (54) have discovered frequent copy number gain of *ALK* in rhabdomyosarcoma accompanied with an increased level of ALK protein. In some cases, *ALK* copy number was even above 10. Interestingly, contrary to neuroblastoma, rhabdomyosarcoma with *ALK* amplification do not carry *MYCN* amplification. Such *ALK* anomaly is likely to be connected to carcinogenesis because *ALK* gain was associated with poor survival and the occurrence of metastases. In addition, van Gaal and colleagues also identified one case with ALK (D1225N) and 7 with *ALK* frameshift mutations of 43 rhabdomyosarcoma specimens, although clinical relevance of such mutations is yet to be examined.

RESISTANCE TO ALK INHIBITORS

Some EML4-ALK–positive NSCLC tumors are insensitive to initial treatment with ALK inhibitors, whereas others acquire resistance to these drugs after initial successful treatment. Information on the molecular mechanisms underlying such resistance remains limited.

The first insight into such resistance mechanisms was provided by analysis of an individual with EML4-ALK–positive NSCLC who initially showed a partial response to crizotinib treatment but underwent a rapid relapse after 5 months. *EML4-ALK* cDNA was amplified by PCR from tumor specimens obtained before the onset of treatment and after relapse, and it was then subjected to deep sequencing with a next-generation sequencer. Comparison of the 2 data sets resulted in the identification of 2 nonsynonymous mutations present only in the latter specimen. Interestingly, these 2 amino acid substitutions (C1156Y and L1196M) were found to independently confer resistance to crizotinib and other ALK inhibitors (55).

Neither C1156Y nor L1196M affects the enzymatic activity of EML4-ALK. NSCLC cells harboring either mutant might therefore be positively selected *in vivo* only in the presence of ALK inhibitors. Furthermore, Leu^{1196} is the "gatekeeper" site buried deeply within the ATP-binding pocket of ALK, with the corresponding sites of EGFR (Thr^{790}) and BCR-ABL1 (Thr^{315}) being the most frequently mutated residues associated with gefitinib and imatinib resistance, respectively (56).

Examination of a similar *EML4-ALK*–positive individual who initially responded to crizotinib but later acquired resistance revealed the presence in post-relapse *EML4-ALK* cDNA of a mutation resulting in an L1152R substitution in the kinase domain (57). Another mutation conferring drug resistance (F1174L) was identified in a case of RANBP2-ALK–positive IMTs (58). Of note, F1174L is also one of the frequent amino acid substitutions identified in neuroblastoma (Fig. 3). Further extensive screening of crizotinib-resistant mutations among 18 relapsed patients revealed 4 secondary mutations (1151Tins, L1196M, G1202R, and S1206Y) within the kinase domain of EML4-ALK, all of which confer resistance to ALK inhibitors (59). Such investigation further identified a high-level amplification of *EML4-ALK* in one patient, suggesting another mechanism (gene amplification) of drug insensitivity.

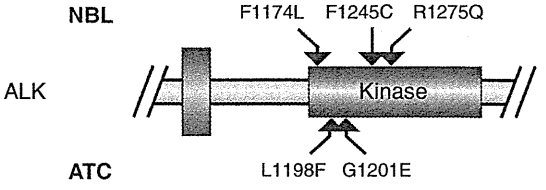

Figure 3. Missense mutations in ALKs. Activating mutations of ALKs are associated with familial and sporadic neuroblastoma (NBL). A different set of missense mutations is also associated with a subset of ATC tumors. Representative mutations for each disorder are shown according to their location in the kinase domain of ALK.

Another screening of *EML4-ALK*–positive tumors at a relapsed phase led to the identification of L1196M (in 2 of 14 resistant cases) and G1269A (in 2 cases) mutations accounting for the acquired drug resistance, and of gene amplification in 2 cases (60). Interestingly, in this cohort, some tumors lost *EML4-ALK* oncogene at the relapsed phase, but instead acquired activating *EGFR* or *KRAS* mutations. Whether such oncogenes other than *EML4-ALK* were present in a minor population of the original tumor or secondarily acquired during the crizotinib treatment remains elusive.

As of March 2012, 5 distinct ALK inhibitors are in clinical trials worldwide (Table 1), with some of these drugs showing inhibitory activity *in vitro* even with the gatekeeper mutant (61, 62). It will thus be of interest to determine whether treatment with such inhibitors results in the development of acquired resistance or not.

ALKOMA: A STEP TOWARD GENETIC INFORMATION–BASED CANCER CLASSIFICATION

Since the initial discovery of NPM1-ALK in 1994, our knowledge of the role of ALK in human cancer has increased markedly. We now recognize the contribution of ALK to an unexpectedly wide range of tumors, with *ALK* translocations underlying lymphoma, lung carcinoma, kidney cancer, and soft tissue tumors and *ALK* mutations being responsible for neuronal and thyroid cancer and *ALK* amplification frequently occurring in rhabdomyosarcoma.

Given that all ALK fusion kinases retain an intact ATP-binding pocket (where most ALK inhibitors bind), it is likely that ALK inhibitors will be effective against any tumor type that harbors such an ALK fusion (63, 64). From the standpoint of pharmaceutical companies, the fact that a single compound can serve as a magic pill for many different types of cancer in different organs is sufficiently compelling to warrant the development of such drugs even if the individual cancer types do not have a high incidence.

For neuroblastoma and ATC, however, the efficacy of an ALK inhibitor may be substantially influenced by the type or position of the missense mutation. However, given that ALK is a transmembrane protein, the mutant proteins may

Published OnlineFirst May 21, 2012; DOI:10.1158/2159-8290.CD-12-0009

be effectively targeted by antibodies (65), as is the case for other transmembrane proteins targeted by the antibodies rituximab and trastuzumab.

Genetic information was first integrated into the classification of hematologic malignancies. For instance, whereas acute myeloid leukemia (AML) had previously been divided into subgroups with distinct differentiation profiles (assessed by pathologic analyses), AML harboring *RUNX1-RUNX1T1*, *PML-RARA*, or *MLL* rearrangements is now defined as a distinct entity according to the current World Health Organization classification (66). Likewise, all-*trans* retinoic acid is highly effective only in the treatment of retinoic acid receptor alpha (encoded by *RARA*) fusion-positive AML, acute promyelocytic leukemia (APL). Similarly, ABL1 inhibitors are only used against *BCR-ABL1*-positive CML/acute lymphoblastic leukemia. It is likely that tumor cells of APL or CML are deeply addicted to the activity of PML-RARA or BCR-ABL1, respectively. Therefore, single reagents targeting individual oncoproteins have a profound therapeutic effect.

In the treatment of epithelial tumors, single EGFR inhibitors provide a high response rate to NSCLCs harboring activating *EGFR* mutations as well. Importantly, treatment with such EGFR inhibitors worsens the prognosis of NSCLC without *EGFR* mutations (67). Targeted drugs are, thus, likely to be highly effective only against tumors in which corresponding targets carry activating mutations and become "essential growth drivers" for the cancer. The definition of essential growth drivers for given oncogenes is difficult because treatment efficacy for cell lines *in vitro* does not always recapitulate that in clinics. For instance, while inhibitors against RAS or PIK3CA are able to suppress the growth of cancer cell lines, these compounds have failed to provide such efficacy in humans.

Therefore, significant response in patients by a monotherapy with a targeted drug should be a faithful indicator for the corresponding target to be the essential growth driver. Unfortunately, however, such clinically proven drivers are still few, but EML4-ALK is a newcomer to this growing list. Importantly, other ALK fusions, NPM1-ALK and RANBP2-ALK, are likely the essential growth drivers as well, because the crizotinib monotherapy has a profound therapeutic effect (63, 64). I propose that these tumors be collectively referred to as "ALKoma," in which abnormal ALK plays an indispensable component in the carcinogenesis.

Interestingly, the term "ALKoma" encompasses multiple organs. NSCLCs, IMTs, and ALCLs were once regarded as completely distinct clinical entities affecting different organs. However, it is now known that a fraction of each of these cancer types shares activated ALK as the essential growth driver and such tumors can be targeted for treatment with ALK inhibitors (32, 63, 64). Because of the similar protein structure to that of EML4-ALK/NPM1-ALK/RANBP2-ALK, VCL-ALK in RMCs should be a good candidate for the next member of ALKoma. Data from ongoing clinical trials with crizotinib for neuroblastoma will also tell us whether activated ALK with nonsynonymous mutations is also a strong driver for this disorder. The term "ALKoma" has the advantage that it indicates the preferred treatment for the tumor. It is thus a good example of genetic information–based "beyond organ" cancer classification, many other examples of which may emerge in the future.

Disclosure of Potential Conflicts of Interest

H. Mano has commercial research grant from Astellas Pharma and Illumina Inc.; Ownership Interest (including patents); and serves as a scientific advisor for Pfizer Inc., Astellas Pharma, Chugai Pharmaceutical, and Daiichi Sankyo Co., Ltd., and is an CEO of CureGene Co., Ltd.

Author's Contributions

Conception and design: H. Mano
Analysis and interpretation of data (e.g., statistical analysis, biostatistics, computational analysis): H. Mano
Writing, review, and/or revision of the manuscript: H. Mano
Study supervision: H. Mano

Acknowledgments

The author apologizes to all the authors whose work could not be included in the manuscript owing to space constraints and also thanks the members of his laboratory as well as K. Takeuchi for their dedication and support.

Grant Support

This work was supported in part by a grant for Research on Human Genome Tailor-made from the Ministry of Health, Labor, and Welfare of Japan as well as by a Grant-in-Aid for Scientific Research on Priority Areas from the Ministry of Education, Culture, Sports, Science, and Technology of Japan.

Received January 6, 2012; revised April 20, 2012; accepted April 20, 2012; published OnlineFirst May 21, 2012.

REFERENCES

1. Morris SW, Naeve C, Mathew P, James PL, Kirstein MN, Cui X, et al. ALK, the chromosome 2 gene locus altered by the t(2;5) in non-Hodgkin's lymphoma, encodes a novel neural receptor tyrosine kinase that is highly related to leukocyte tyrosine kinase (LTK). Oncogene 1997;14:2175–88.
2. Iwahara T, Fujimoto J, Wen D, Cupples R, Bucay N, Arakawa T, et al. Molecular characterization of ALK, a receptor tyrosine kinase expressed specifically in the nervous system. Oncogene 1997;14:439–49.
3. Beckmann G, Bork P. An adhesive domain detected in functionally diverse receptors. Trends Biochem Sci 1993;18:40–1.
4. Pulford K, Lamant L, Morris SW, Butler LH, Wood KM, Stroud D, et al. Detection of anaplastic lymphoma kinase (ALK) and nucleolar protein nucleophosmin (NPM)-ALK proteins in normal and neoplastic cells with the monoclonal antibody ALK1. Blood 1997;89:1394–404.
5. Bilsland JG, Wheeldon A, Mead A, Znamenskiy P, Almond S, Waters KA, et al. Behavioral and neurochemical alterations in mice deficient in anaplastic lymphoma kinase suggest therapeutic potential for psychiatric indications. Neuropsychopharmacology 2008;33:685–700.
6. Lasek AW, Lim J, Kliethermes CL, Berger KH, Joslyn G, Brush G, et al. An evolutionary conserved role for anaplastic lymphoma kinase in behavioral responses to ethanol. PLoS One 2011;6:e22636.
7. Lee HH, Norris A, Weiss JB, Frasch M. Jelly belly protein activates the receptor tyrosine kinase Alk to specify visceral muscle pioneers. Nature 2003;425:507–12.
8. Stoica GE, Kuo A, Aigner A, Sunitha I, Souttou B, Malerczyk C, et al. Identification of anaplastic lymphoma kinase as a receptor for the growth factor pleiotrophin. J Biol Chem 2001;276:16772–9.
9. Stoica GE, Kuo A, Powers C, Bowden ET, Sale EB, Riegel AT, et al. Midkine binds to anaplastic lymphoma kinase (ALK) and acts as a growth factor for different cell types. J Biol Chem 2002;277:35990–8.
10. Mathivet T, Mazot P, Vigny M. In contrast to agonist monoclonal antibodies, both C-terminal truncated form and full length form of Pleiotrophin failed to activate vertebrate ALK (anaplastic lymphoma kinase)? Cell Signal 2007;19:2434–43.

Published OnlineFirst May 21, 2012; DOI:10.1158/2159-8290.CD-12-0009

11. Morris SW, Kirstein MN, Valentine MB, Dittmer KG, Shapiro DN, Saltman DL, et al. Fusion of a kinase gene, ALK, to a nucleolar protein gene, NPM, in non-Hodgkin's lymphoma. Science 1994;263:1281–4.
12. Shiota M, Fujimoto J, Semba T, Satoh H, Yamamoto T, Mori S. Hyperphosphorylation of a novel 80 kDa protein-tyrosine kinase similar to Ltk in a human Ki-1 lymphoma cell line, AMS3. Oncogene 1994;9:1567–74.
13. Pulford K, Lamant L, Espinos E, Jiang Q, Xue L, Turturro F, et al. The emerging normal and disease-related roles of anaplastic lymphoma kinase. Cell Mol Life Sci 2004;61:2939–53.
14. Lawrence B, Perez-Atayde A, Hibbard MK, Rubin BP, Dal Cin P, Pinkus JL, et al. TPM3-ALK and TPM4-ALK oncogenes in inflammatory myofibroblastic tumors. Am J Pathol 2000;157:377–84.
15. Jazii FR, Najafi Z, Malekzadeh R, Conrads TP, Ziaee AA, Abnet C, et al. Identification of squamous cell carcinoma associated proteins by proteomics and loss of beta tropomyosin expression in esophageal cancer. World J Gastroenterol 2006;12:7104–12.
16. Sugawara E, Togashi Y, Kuroda N, Sakata S, Hatano S, Asaka R, et al. Identification of anaplastic lymphoma kinase fusions in renal cancer: large-scale immunohistochemical screening by the intercalated antibody-enhanced polymer method. Cancer. 2012 Jan 7. [Epub ahead of print]
17. Soda M, Choi YL, Enomoto M, Takada S, Yamashita Y, Ishikawa S, et al. Identification of the transforming *EML4-ALK* fusion gene in non-small-cell lung cancer. Nature 2007;448:561–6.
18. Mosse YP, Laudenslager M, Longo L, Cole KA, Wood A, Attiyeh EF, et al. Identification of ALK as a major familial neuroblastoma predisposition gene. Nature 2008;455:930–5.
19. Janoueix-Lerosey I, Lequin D, Brugieres L, Ribeiro A, de Pontual L, Combaret V, et al. Somatic and germline activating mutations of the ALK kinase receptor in neuroblastoma. Nature 2008;455:967–70.
20. George RE, Sanda T, Hanna M, Frohling S, Luther W II, Zhang J, et al. Activating mutations in ALK provide a therapeutic target in neuroblastoma. Nature 2008;455:975–8.
21. Chen Y, Takita J, Choi YL, Kato M, Ohira M, Sanada M, et al. Oncogenic mutations of ALK kinase in neuroblastoma. Nature 2008;455:971–4.
22. Barreca A, Lasorsa E, Riera L, Machiorlatti R, Piva R, Ponzoni M, et al. Anaplastic lymphoma kinase in human cancer. J Mol Endocrinol 2011;47:R11–23.
23. Pulford K, Morris SW, Turturro F. Anaplastic lymphoma kinase proteins in growth control and cancer. J Cell Physiol 2004;199:330–58.
24. Druker BJ, Talpaz M, Resta DJ, Peng B, Buchdunger E, Ford JM, et al. Efficacy and safety of a specific inhibitor of the BCR-ABL tyrosine kinase in chronic myeloid leukemia. N Engl J Med 2001;344:1031–7.
25. Tomlins SA, Rhodes DR, Perner S, Dhanasekaran SM, Mehra R, Sun XW, et al. Recurrent fusion of TMPRSS2 and ETS transcription factor genes in prostate cancer. Science 2005;310:644–8.
26. Choi YL, Takeuchi K, Soda M, Inamura K, Togashi Y, Hatano S, et al. Identification of novel isoforms of the *EML4-ALK* transforming gene in non-small cell lung cancer. Cancer Res 2008;68:4971–6.
27. Koivunen JP, Mermel C, Zejnullahu K, Murphy C, Lifshits E, Holmes AJ, et al. EML4-ALK fusion gene and efficacy of an ALK kinase inhibitor in lung cancer. Clin Cancer Res 2008;14:4275–83.
28. Soda M, Takada S, Takeuchi K, Choi YL, Enomoto M, Ueno T, et al. A mouse model for *EML4-ALK*-positive lung cancer. Proc Natl Acad Sci U S A 2008;105:19893–7.
29. Chen Z, Sasaki T, Tan X, Carretero J, Shimamura T, Li D, et al. Inhibition of ALK, PI3K/MEK, and HSP90 in murine lung adenocarcinoma induced by EML4-ALK fusion oncogene. Cancer Res 2010;70:9827–36.
30. Takeuchi K, Choi YL, Soda M, Inamura K, Togashi Y, Hatano S, et al. Multiplex reverse transcription-PCR screening for EML4-ALK fusion transcripts. Clin Cancer Res 2008;14:6618–24.
31. Wong DW, Leung EL, So KK, Tam IY, Sihoe AD, Cheng LC, et al. The EML4-ALK fusion gene is involved in various histologic types of lung cancers from nonsmokers with wild-type EGFR and KRAS. Cancer 2009;115:1723–33.
32. Kwak EL, Bang YJ, Camidge DR, Shaw AT, Solomon B, Maki RG, et al. Anaplastic lymphoma kinase inhibition in non-small-cell lung cancer. N Engl J Med 2010;363:1693–703.
33. Tiseo M, Gelsomino F, Boggiani D, Bortesi B, Bartolotti M, Bozzetti C, et al. EGFR and EML4-ALK gene mutations in NSCLC: a case report of erlotinib-resistant patient with both concomitant mutations. Lung Cancer 2011;71:241–3.
34. Takeuchi K, Choi YL, Togashi Y, Soda M, Hatano S, Inamura K, et al. KIF5B-ALK, a novel fusion oncokinase identified by an immunohistochemistry-based diagnostic system for ALK-positive lung cancer. Clin Cancer Res 2009;15:3143–9.
35. Mino-Kenudson M, Chirieac LR, Law K, Hornick JL, Lindeman N, Mark EJ, et al. A novel, highly sensitive antibody allows for the routine detection of ALK-rearranged lung adenocarcinomas by standard immunohistochemistry. Clin Cancer Res 2010;16:1561–71.
36. Yoshida A, Tsuta K, Nakamura H, Kohno T, Takahashi F, Asamura H, et al. Comprehensive histologic analysis of ALK-rearranged lung carcinomas. Am J Surg Pathol 2011;35:1226–34.
37. Lin E, Li L, Guan Y, Soriano R, Rivers CS, Mohan S, et al. Exon array profiling detects EML4-ALK fusion in breast, colorectal, and non-small cell lung cancers. Mol Cancer Res 2009;7:1466–76.
38. Sanders HR, Li HR, Bruey JM, Scheerle JA, Meloni-Ehrig AM, Kelly JC, et al. Exon scanning by reverse transcriptase-polymerase chain reaction for detection of known and novel EML4-ALK fusion variants in non-small cell lung cancer. Cancer Genet 2011;204:45–52.
39. Christensen JG, Zou HY, Arango ME, Li Q, Lee JH, McDonnell SR, et al. Cytoreductive antitumor activity of PF-2341066, a novel inhibitor of anaplastic lymphoma kinase and c-Met, in experimental models of anaplastic large-cell lymphoma. Mol Cancer Ther 2007;6:3314–22.
40. Shaw AT, Yeap BY, Solomon BJ, Riely GJ, Gainor J, Engelman JA, et al. Effect of crizotinib on overall survival in patients with advanced non-small-cell lung cancer harbouring ALK gene rearrangement: a retrospective analysis. Lancet Oncol 2011;12:1004–12.
41. Engelman JA, Zejnullahu K, Mitsudomi T, Song Y, Hyland C, Park JO, et al. MET amplification leads to gefitinib resistance in lung cancer by activating ERBB3 signaling. Science 2007;316:1039–43.
42. Bergethon K, Shaw AT, Ignatius Ou SH, Katayama R, Lovly CM, McDonald NT, et al. ROS1 rearrangements define a unique molecular class of lung cancers. J Clin Oncol 2012;30:863–70.
43. Takeuchi K, Soda M, Togashi Y, Suzuki R, Sakata S, Hatano S, et al. RET, ROS1 and ALK fusions in lung cancer. Nat Med 2012;18:378–81.
44. Gerber DE, Minna JD. ALK inhibition for non-small cell lung cancer: from discovery to therapy in record time. Cancer Cell 2010;18:548–51.
45. Wong DW, Leung EL, Wong SK, Tin VP, Sihoe AD, Cheng LC, et al. A novel KIF5B-ALK variant in nonsmall cell lung cancer. Cancer 2011;117:2709–18.
46. Togashi Y, Soda M, Sakata S, Sugawara E, Hatano S, Asaka R, et al. KLC1-ALK: a novel fusion in lung cancer identified using a formalin-fixed paraffin-embedded tissue only. PLoS One 2012;7:e31323.
47. Debelenko LV, Raimondi SC, Daw N, Shivakumar BR, Huang D, Nelson M, et al. Renal cell carcinoma with novel VCL-ALK fusion: new representative of ALK-associated tumor spectrum. Mod Pathol 2011;24:430–42.
48. Marino-Enriquez A, Ou WB, Weldon CB, Fletcher JA, Perez-Atayde AR. ALK rearrangement in sickle cell trait-associated renal medullary carcinoma. Genes Chromosomes Cancer 2011;50:146–53.
49. Bresler SC, Wood AC, Haglund EA, Courtright J, Belcastro LT, Plegaria JS, et al. Differential inhibitor sensitivity of anaplastic lymphoma kinase variants found in neuroblastoma. Sci Transl Med 2011;3:108ra14.
50. Schonherr C, Ruuth K, Yamazaki Y, Eriksson T, Christensen J, Palmer RH, et al. Activating ALK mutations found in neuroblastoma are inhibited by crizotinib and NVP-TAE684. Biochem J 2011;440:405–13.
51. Schonherr C, Ruuth K, Eriksson T, Yamazaki Y, Ottmann C, Combaret V, et al. The neuroblastoma ALK(I1250T) mutation is a kinase-dead RTK *in vitro* and *in vivo*. Transl Oncol 2011;4:258–65.
52. Murugan AK, Xing M. Anaplastic thyroid cancers harbor novel oncogenic mutations of the ALK gene. Cancer Res 2011;71:4403–11.
53. Bagci O, Tumer S, Olgun N, Altungoz O. Copy number status and mutation analyses of anaplastic lymphoma kinase (ALK) gene in 90 sporadic neuroblastoma tumors. Cancer Lett 2012;317:72–7.

Published OnlineFirst May 21, 2012; DOI:10.1158/2159-8290.CD-12-0009

54. van Gaal JC, Flucke UE, Roeffen MH, de Bont ES, Sleijfer S, Mavinkurve-Groothuis AM, et al. Anaplastic lymphoma kinase aberrations in rhabdomyosarcoma: clinical and prognostic implications. J Clin Oncol 2012;30:308–15.
55. Choi YL, Soda M, Yamashita Y, Ueno T, Takashima J, Nakajima T, et al. EML4-ALK mutations in lung cancer that confer resistance to ALK inhibitors. N Engl J Med 2010;363:1734–9.
56. Carter TA, Wodicka LM, Shah NP, Velasco AM, Fabian MA, Treiber DK, et al. Inhibition of drug-resistant mutants of ABL, KIT, and EGF receptor kinases. Proc Natl Acad Sci U S A 2005;102:11011–6.
57. Sasaki T, Koivunen J, Ogino A, Yanagita M, Nikiforow S, Zheng W, et al. A novel ALK secondary mutation and EGFR signaling cause resistance to ALK kinase inhibitors. Cancer Res 2011;71:6051–60.
58. Sasaki T, Okuda K, Zheng W, Butrynski J, Capelletti M, Wang L, et al. The neuroblastoma-associated F1174L ALK mutation causes resistance to an ALK kinase inhibitor in ALK-translocated cancers. Cancer Res 2010;70:10038–43.
59. Katayama R, Shaw AT, Khan TM, Mino-Kenudson M, Solomon BJ, Halmos B, et al. Mechanisms of acquired crizotinib resistance in ALK-rearranged lung cancers. Sci Transl Med 2012;4:120ra17.
60. Doebele RC, Pilling AB, Aisner DL, Kutateladze TG, Le AT, Weickhardt AJ, et al. Mechanisms of resistance to crizotinib in patients with ALK gene rearranged non-small cell lung cancer. Clin Cancer Res 2012;18:1472–82.
61. Katayama R, Khan TM, Benes C, Lifshits E, Ebi H, Rivera VM, et al. Therapeutic strategies to overcome crizotinib resistance in non-small cell lung cancers harboring the fusion oncogene EML4-ALK. Proc Natl Acad Sci U S A 2011;108:7535–40.
62. Sakamoto H, Tsukaguchi T, Hiroshima S, Kodama T, Kobayashi T, Fukami TA, et al. CH5424802, a selective ALK inhibitor capable of blocking the resistant gatekeeper mutant. Cancer Cell 2011;19:679–90.
63. Butrynski JE, D'Adamo DR, Hornick JL, Dal Cin P, Antonescu CR, Jhanwar SC, et al. Crizotinib in ALK-rearranged inflammatory myofibroblastic tumor. N Engl J Med 2010;363:1727–33.
64. Gambacorti-Passerini C, Messa C, Pogliani EM. Crizotinib in anaplastic large-cell lymphoma. N Engl J Med 2011;364:775–6.
65. Wellstein A, Toretsky JA. Hunting ALK to feed targeted cancer therapy. Nat Med 2011;17:290–1.
66. Vardiman JW, Thiele J, Arber DA, Brunning RD, Borowitz MJ, Porwit A, et al. The 2008 revision of the World Health Organization (WHO) classification of myeloid neoplasms and acute leukemia: rationale and important changes. Blood 2009;114:937–51.
67. Mok TS, Wu YL, Thongprasert S, Yang CH, Chu DT, Saijo N, et al. Gefitinib or carboplatin-paclitaxel in pulmonary adenocarcinoma. N Engl J Med 2009;361:947–57.
68. Zou HY, Li Q, Lee JH, Arango ME, McDonnell SR, Yamazaki S, et al. An orally available small-molecule inhibitor of c-Met, PF-2341066, exhibits cytoreductive antitumor efficacy through antiproliferative and antiangiogenic mechanisms. Cancer Res 2007;67:4408–17.

Lung Cancer 75 (2012) 66–72

Contents lists available at ScienceDirect

Lung Cancer

journal homepage: www.elsevier.com/locate/lungcan

ALK fusion gene positive lung cancer and 3 cases treated with an inhibitor for ALK kinase activity

Hideki Kimura[a,*], Takahiro Nakajima[a,d], Kengo Takeuchi[b], Manabu Soda[c], Hiroyuki Mano[c], Toshihiko Iizasa[a], Yukiko Matsui[a], Mitsuru Yoshino[a], Masato Shingyoji[a], Meiji Itakura[a], Makiko Itami[e], Dai Ikebe[e], Sana Yokoi[f], Hajime Kageyama[f], Miki Ohira[g], Akira Nakagawara[h]

[a] Division of Thoracic Diseases, Chiba Cancer Center, Chiba, Japan
[b] Pathology Project for Molecular Targets, Cancer Institute, Japanese Foundation for Cancer Research (JFCR), Koto, Tokyo, Japan
[c] Division of Functional Genomics, Jichi Medical University, Tochigi, Japan
[d] Division of Thoracic Surgery, Toronto General Hospital, University Health Network, Toronto, Canada
[e] Division of Pathology, Chiba Cancer Center, Japan
[f] Cancer Genome Center, Chiba Cancer Center Research Institute, Japan
[g] Laboratory of Cancer Genomics, Chiba Cancer Center Research Institute, Japan
[h] Chiba Cancer Center, Japan

ARTICLE INFO

Article history:
Received 16 October 2010
Received in revised form 24 May 2011
Accepted 30 May 2011

Key words:
ALK
EML4
KIF5B
Fusion gene
Lung cancer
EBUS
TBNA
Crizotinib
ALK inhibitor

ABSTRACT

Background: Anaplastic lymphoma kinase (ALK) fusion gene-positive lung cancer accounts for 4–5% of non-small cell lung carcinoma. A clinical trial of the specific inhibitor of ALK fusion-type tyrosine kinase is currently under way.
Methods: ALK fusion gene products were analyzed immunohistochemically with the materials obtained by surgery or by endobronchial ultrasound-guided transbronchial needle aspiration (EBUS-TBNA). The echinoderm microtubule-associated protein-like 4(EML4)-ALK or kinesin family member 5B (KIF5B)-ALK translocation was confirmed by the reverse transcription polymerase chain reaction (RT-PCR) and fluorescence in situ hybridization (FISH). After eligibility criteria were met and informed consent was obtained, 3 patients were enrolled for the Pfizer Study of Crizotinib (PF02341066), Clinical Trial A8081001, conducted at Seoul National University.
Results: Out of 404 cases, there were 14 of EML4-ALK non-small cell carcinoma (NSCLC) and one KIF5B-ALK NSCLC case (8 men, 7 women; mean age, 61.9 years, range 48–82). Except for 2 light smokers, all patients were non-smokers. All cases were of adenocarcinoma with papillary or acinar subtypes. Three were of stage IA, 5 of stage IIIA, 1 of stage IIIB and 6 of stage IV. Ten patients underwent thoracotomy, 3 received chemotherapy and 2 only best supportive care (BSC). One BSC and 2 chemotherapy cases were enrolled for the clinical trial. Patients with advanced stages who received chemotherapy or best supportive care were younger (54.0 ± 6.3) than those who were surgically treated (65.8 ± 10.1) ($p < 0.05$).
The powerful effect of ALK inhibitor on EML4-ALK NSCLC was observed. Soon after its administration, almost all the multiple bone and lymph node metastases quickly disappeared. Nausea, diarrhea and the persistence of a light image were the main side effects, but they diminished within a few months.
Conclusion: ALK-fusion gene was found in 3.7% (15/404) NSCLC cases and advanced disease with this fusion gene was correlated with younger generation. The ALK inhibitor presented in this study is effective in EML4-ALK NSCLC cases. A further study will be necessary to evaluate the clinical effectiveness of this drug.

1. Introduction

As the mechanisms of carcinogenesis become clearer, the target of cancer treatment is shifting from non-specific cytotoxic agents to specific agents that block key molecular events in the carcinogenesis of malignancy such as EGFR-TKI and anti-HER2 antibody (trastuzumab) [1–3]. Recently, Mano et al. [4–6] reported that a small inversion within chromosome 2p results in the formation of a fusion gene comprising portions of the

* Corresponding author at: Division of Thoracic Diseases, Chiba Cancer Center, 666-2, Nitona-cho, Chuo-ku, 260-8717 Chiba, Japan. Tel.: +81 43 264 5431; fax: +81 43 262 8680.
E-mail address: hkimura@chiba-cc.jp (H. Kimura).

0169-5002/$ – see front matter © 2011 Elsevier Ireland Ltd. All rights reserved.
doi:10.1016/j.lungcan.2011.05.027

echinoderm microtubule-associated protein-like 4 (EML4) gene and the anaplastic lymphoma kinase (ALK) gene in non-small-cell lung cancer. Transgenic mice that express EML4-ALK specifically in lung epithelial cells develop multiple foci of adenocarcinoma in the lung soon after birth, and the oral administration of a specific inhibitor of ALK tyrosine kinase activity eradicated completely the foci of adenocarcinoma. Clinical trials of specific inhibitors of EML4-ALK tumors are currently underway [7–11]. Kwak et al. [11] reported the effect of crizotinib in Clinical Trial A8081001 on the 82 patients with advanced ALK-positive disease. Over a mean treatment duration of 6.4 months, the overall response rate was 57% and the estimated probability of 6-month progression-free survival was 72%. We report 15 cases of ALK fusion gene-positive NSCLC cases and 3 cases in our experience with ALK inhibitor in the Pfizer Study of crizotinib (PF02341066), Clinical Trial A8081001, which was conducted at Seoul National University.

2. Materials and methods

Out of 404 patients who had undergone surgical resection (295 cases) or bronchoscopy (109 cases) in Chiba Cancer Center, Japan, from 2007 to 2009, 15 ALK fusion gene-positive NSCLC patients were initially screened by immunohistochemical procedures. Diagnoses were confirmed by RT-PCR and/or FISH for their molecular translocation.

2.1. ALK fusion protein detection by immunohistochemical methods

The intercalated antibody-enhanced polymer method of Takeuchi et al. [12,13] was used to detect ALK proteins. Formalin-fixed paraffin-embedded tissue was sliced at a thickness of 4 μm and the sections were placed on silane-coated slides. For antigen retrieval, the slides were heated for 40 min at 97 °C in target Retrieval Solution (pH 9.0; Dako). They were then incubated at room temperature, first with Protein Block Serum-free Ready-to-Use solution (Dako) for 10 min, and then with an anti-ALK antibody (5A4, Abcam) for 30 min. To increase the sensitivity of detection, we included an incubation step of 15 min at room temperature with rabbit polyclonal antibodies to mouse immunoglobulin (Dako). The immune complexes were then detected with the dextran polymer reagent and an AutoStainer instrument (Dako).

2.2. Confirmation of EML4-ALK fusion gene by RT-PCR and FISH

We confirmed the existence of ALK fusion gene expression by fluorescence in situ hybridization (FISH) and/or by the reverse transcription-polymerase chain reaction (RT-PCR).

2.3. Fluorescence in situ hybridization (FISH)

An EML4-ALK fusion assay was performed [10–12]. Unstained sections were processed with a Histology FISH Accessory Kit (Dako), subjected to hybridization with fluorescence-labeled bacterial artificial chromosome clone probes for EML4 and ALK (self-produced probes; EML4: RP11-996L7, ALK: RP11-984I21 and RP11-62B19), stained with 4,6-diamidino-2-phenylindole, and examined with a fluorescence microscope (BX51; Olympus). The FISH positivity criteria specified "over 50% cancer cells" for EBUS-TBNA samples.

2.4. Reverse transcription-polymerase chain reaction (RT-PCR)

The multiplex PCR method proposed by the Japanese ALK lung cancer study group (ALCAS) was used to confirm the expression of ALK fusion gene [4–6].

Table 1
Characteristics of ALK fusion gene positive lung cancer patients.

Patient no	Sex	Age	SI	Histology	Variant	p Stage	Therapy	Recurrence	Distant meta	Survival (M)	Prognosis	ALK inhibitor case no
1	f	64	0	Ad: papillary	3	IIIA	Surgery	Positive	Bone, brain	21	Dead	
2	m	82	0	Ad: solid	2	IIIA	Surgery	Positive	Ascites	36	Alive	
3	f	68	0	Ad: papillary	3	IIIB	Surgery	Positive	Brain	34	Alive	
4	f	60	0	Ad: solid	3	IIIA	Surgery	Negative	None	29	Alive	
5	m	73	0	Ad: acinar	3	IA	Surgery	Negative	None	21	Alive	
6	m	66	0	Ad: papillary	KIF5B	IA	Surgery	Negative	None	15	Alive	
7	m	56	300	Ad: papillary	1	IA	Surgery	Negative	None	13	Alive	
8	m	46	0	Ad: acinar	5	IIIA	Surgery	Negative	None	22	Alive	
9	m	71	0	Ad: papillary	1	IIIA	Surgery	Negative		17	Alive	
10	f	73	0	Ad: acinar	1	IV	Surgery	Negative		14	Alive	
11	m	55	100	Ad: muc+	3	IV	BSC		Bone, brain	5	Dead	
12	m	48	0	Ad: muc+	1	IV	Chemo		Bone, brain	29	Dead	Case 1
13	f	49	0	Ad: muc+	3	IV	BSC		Bone, brain	15	Alive	Case 2
14	f	54	0	Ad: muc+	1	IV	Chemo		Bone, brain, pul	22	Alive	Case 3
15	f	64	0	Ad: acinar	3	IV	Chemo		Pul	2	Alive	

SI, smoking index; f, female; m, male; Ad, adenocarcinoma; muc+, mucin production; Distant meta, at the recurrence (surgery group) at the diagnosis (non-surgery group); pul, pulmonary metastasis; Case 1 was already reported by Nakajima et al. [16].

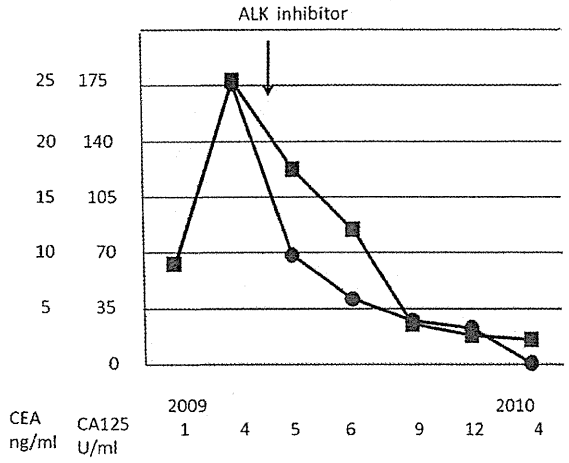

Fig. 1. Changes of tumor markers before and during the treatment with ALK inhibitor (Case 1) CEA (■), CA125 (●). Marked reduction of tumor markers was observed.

Total RNA was isolated from EBUS-TBNA or surgical samples using AllPrep DNA/RNA Mini Kit (Qiagen) and was reverse-transcribed into single strand cDNA using a High Capacity RNA-to-cDNA Kit (Applied Biosystems). To detect a fusion cDNA derived from EML4 or KIF5B and ALK, PCR analysis was performed with the AmpliTaq Gold PCR Master Mix (Applied Biosystems), the forward primers derived from EML4, EA-F-cDNA-S (5′-GTGCAGTGTTTAGCATTCTTGGGG-3′), EA-F-2-g-S (5′-AGCTACATCACACACCTTGACTGG-3′), EA-F-cDNA-v3-S-2 (5′-TACCAGTGCTGTCTCAATTGCAGG-3″) and EA-W-cDNA-in-S (5′-GCTTTCCCCGCAAGATGGACGG-3′) and the forward primers derived from KIF5B, KA-F-cDNA-S-e24 (5′-CAGCTGAGAGAGTGAAAGCTTTGG-3′), KA-F-cDNA-S-e17 (5′-GACAGTTGGAGGAATCTGTCGATG-3′), KA-F-cDNA-S-e11 (5′-ATCCTGCGGAACACTATTCAGTGG-3′), and KA-cDNA-S-e2 (5′-TCAAGCACATCTCAAGAGCAAGTG-3′) and the reverse primer derived from ALK, EA-F-cDNA-A (5′-TCTTGCCAGCAAAG-CAGTAGTTGG-3′). PCR products were purified from gel bands using QIAquick Gel Extraction Kit (Qiagen) and confirmed by direct sequencing analysis.

2.5. Enrolment of patients for the Clinical Trial A8081001

Informed consent was obtained from each patient to be enrolled for the study [10]. Eligibility criteria for the enrolment of ALK translocation positive patients into the ALK TKI PI Trial were as required by the Committee of Clinical Trials A8081001.

3. Results

There were 15 ALK fusion gene-positive cases which were screened immunohistochemically and confirmed by RT-PCR and FISH [14,15]. Eight patients were men and 7 women, of mean age

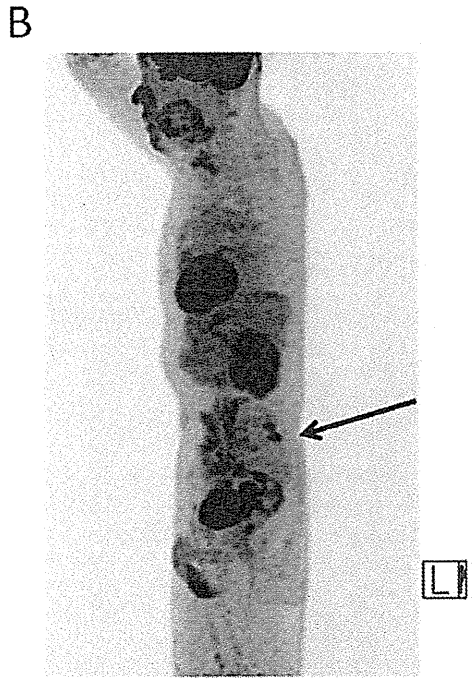

Fig. 2. FDG-PET scan of Case 1 performed at the same time (09/28/2009) as the previously reported Fig. 1D (Nakajima et al. [16]) shows bone metastasis of the left vertebral arch of L5 (arrow) in a sagittal view.

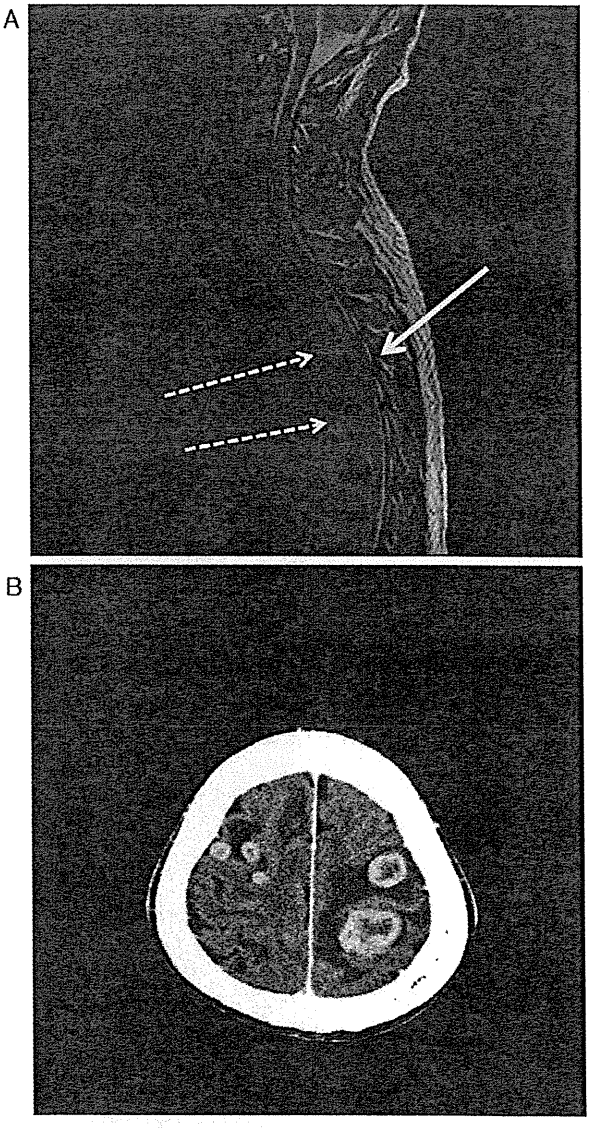

Fig. 3. MRI (Case 1) of the spinal cord on 04/05/2010 shows the metastases to the spinal cord (straight allow) and the spinal column (Th 4,6 dotted allow). B. CT scan (Case 1) of the brain on 04/05/2010 shows multiple brain metastases.

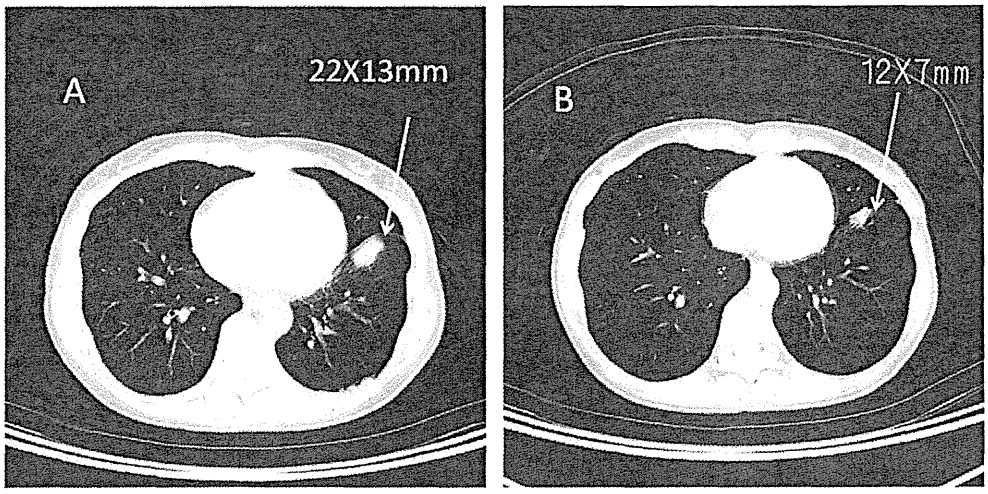

Fig. 4. CT scan (Case 2): A, 07/22/2009 (before ALK inhibitor) and B, 09/02/2009 (5 weeks after the initiation of the therapy). Left S8 tumor (arrow) decreased in size from 22X13 mm to 12X7 mm (PR).

61.9 years (range 48–82). Most were non-smokers, but 2 smoked lightly (Table 1). All tumors were adenocarcinomas with a papillary pattern predominant (5 cases), an acinar pattern predominant (3 cases), with mucin production (4 cases), etc. There were fourteen cases of fusion with EML4 and one KIF5B gene. There were 7 variant 3, 5 variant 1, and 1 each of variants 2 and 5. There were 3 stage IA, 5 stage IIIA, 1 stage IIIB and 6 stage IV cases. Ten cases were diagnosed after surgical resection, and 5, by tissue samples obtained with EBUS-TBNA. Ten cases underwent thoracotomy, 3 cases, chemotherapy, and 2 cases, only best supportive care. Of 5 cases diagnosed by EBUS-TBNA, 2 cases receiving chemotherapy and one receiving best supportive care were enrolled for the clinical trial. The mean age of the surgically treated group was 65.8 ± 10.1, and that of chemotherapy and BSC group was 54.0 ± 6.3. The difference was found by Student's t test to be statistically significant ($p < 0.05$), indicating that younger patients tend to have advanced cancer.

Out of 10 surgically treated cases, seven survived without a sign of recurrence, 3 had recurrence in both bone and brain tissue, and one died of bone and lymph node metastasis.

3.1. Case 1

Case 1 has already been reported in a case report (Nakajima et al.) [16] but without precise descriptions of the response to crizotinib, the adverse effects, the pattern of recurrence or the metastatic

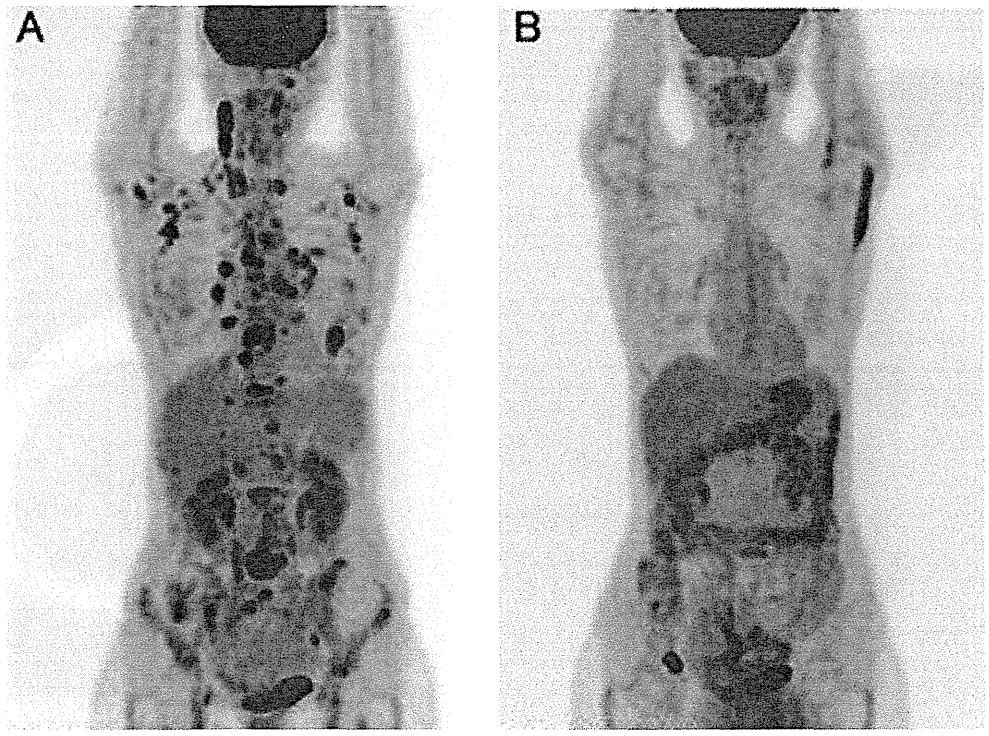

Fig. 5. FDG-PET scan (Case 2): A, 07/22/2009 (before ALK inhibitor) and B, 03/10/2010 FDG-PET scan shows marked reduction of accumulation in multiple bone and lymph node metastases 7 months after the initiation of the treatment.

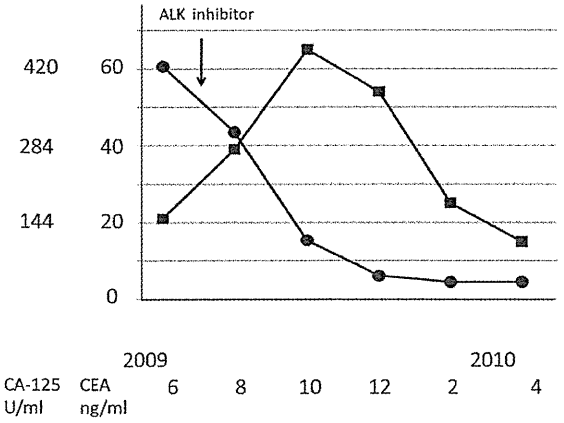

Fig. 6. Changes of tumor markers before and during the treatment with ALK inhibitor in case 2. CA125 (●) gradually decreased along with the treatment, but CEA (■) increased soon after the initiation of the therapy. The value of CEA then gradually decreased to 15.2 ng/ml in April 2010 (after 10 months).

Fig. 7. Brain MRI of case 2 on 7/30/2010 showing multiple metastases.

tumor lesions. Such descriptions may contribute to a better understanding of the other cases, and so case 1 is described briefly below.

A 48-year-old non-smoking male patient had lung adenocarcinoma in the right lower lobe and multiple bone and lymph node metastases (T3N2M1 stage IV) at his first medical examination in November 2007. After several courses of chemotherapy, the patient was enrolled in a trial of crizotinib (PF02341066) from May 5th 2009 at Seoul National University, in which the drug was orally administered at 500 mg/day.

The effect of ALK inhibitor appeared rapidly. The patient's dyspnea improved within one week after drug administration. PS improved from 2 to 0 and a marked reduction in the tumor markers was observed (Fig. 1). Within 3 months after the start of therapy, almost all metastases disappeared except for those at the left vertebral arch of L5 (Fig. 2, arrow). The patient had severe adverse effects: diarrhea, nausea and persistence of light images started soon after the administration of the drug, but these gradually diminished over a 3-week period.

The control of the primary and metastatic tumors continued for 11 months until the patient visited Seoul University in April 2010, when he was hospitalized for paralysis of the lower extremities. MRI revealed spinal column (Th4-6) and spinal cord metastases (Fig. 3A). Soon after his hospitalization in our Cancer Center in April 2010, multiple brain metastases (Fig. 3B) were found, so the drug administration was stopped and he was transferred to a palliative care unit.

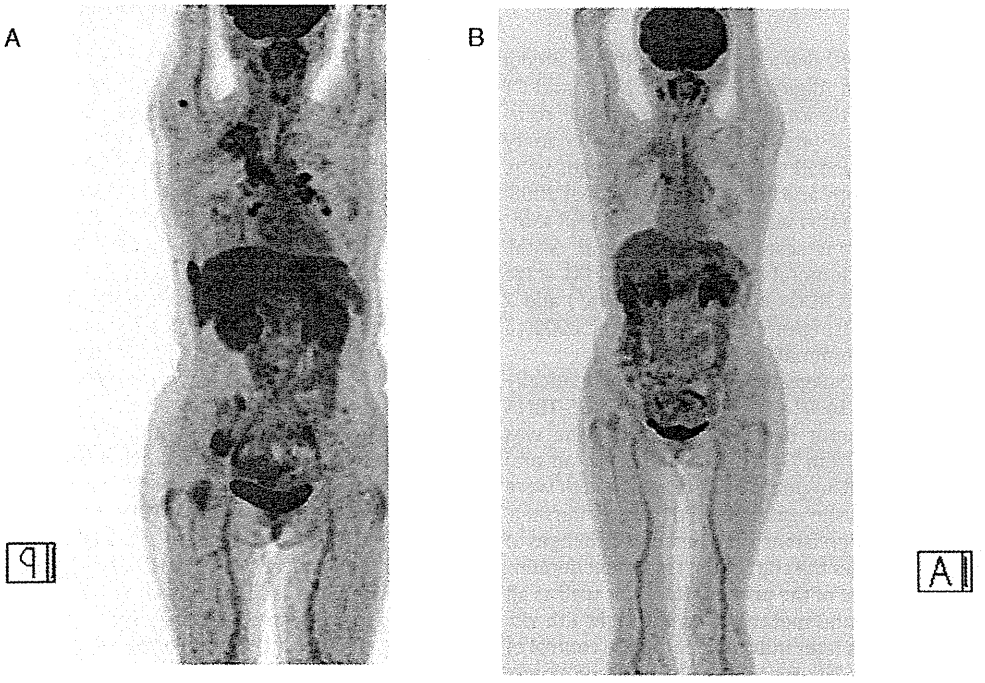

Fig. 8. FDG-PET scan: A, 09/08/2009 (before ALK inhibitor) and B, 07/05/2010 FDG-PET scan follow-up for 10 months indicated complete control of primary and distant metastases in case 3.

3.2. Case 2

A 49-year-old woman, a non-smoker with no history of illness, PS0, was introduced to the Orthopedics Department of our Center in April 2009 for back pain and multiple osteoplastic changes in the bones. Systematic examination revealed an abnormal shadow 22X13 mm in size in the left lower lobe (Fig. 4A). Bronchoscopy and a PET scan indicated left S8 adenocarcinoma with cervical, axial, mediastinal, hilar, pancreatic and retroperitoneal lymph node metastases, as well as cranial, thoracic (Th1-12), lumbar (L1-5), rib (1–12) pelvis, humerus, and femur metastases (Fig. 5A).

She refused any therapy except for best supportive care. One month after the examination, an additional immunohistochemical examination for EML4-ALK fusion protein was performed, and found to be positive. The presence of mRNA for EML4-ALK gene was also confirmed by RT-PCR and FISH from the mediastinal #4R lymph nodes obtained with EBUS-TBNA, which was performed 2 months later. EGFR mutation was negative, but the direct sequence of the EML4-ALK mRNA indicated that the translocation was variant 3 [9]. She decided to be enrolled to the crizotinib study (PF02341066) at a dosage of 500 mg/day at Seoul National University from July 2009.

She had nausea, diarrhea and light image persistence as in case 1, but her gastrointestinal symptoms were severer than those in case 1. Two weeks after the administration of ALK inhibitor, her back pain disappeared. A PET scan performed 5 weeks after the initiation of the therapy showed marked reduction of bone and lymph node metastases, and the primary tumor had decreased in size from 22X13 mm to 12X7 mm (Fig. 4A and B). Also, the SUV max dropped from 10.7 to 2.42. Changes of tumor markers were not parallel with the clinical course since the measured value of CA-125 dropped from 424 to 107 U/ml, but that of CEA increased from 21.5 to 65.4 ng/ml 4 months later. The value of CEA then gradually decreased to 15.2 ng/ml in April 2010 (10 months after that: Fig. 6). The PET scan conducted after 7 months indicated a partial response to multiple bone and lymph node metastases (Fig. 5B). The patient continued to take the drug until the end of July 2010, when brain metastases (Fig. 7) were found.

3.3. Case 3

A fifty-four-year-old woman, also a non-smoker, PS0, visited a doctor because of back pain in August 2008. Chest X-ray and CT scan showed an S3 59X22 mm tumor in the right upper lobe, combined with #4R, #2R mediastinal lymph nodes and intrapulmonary metastases. The tumor had invaded the SVC and the azygos vein. She had undergone bronchoscopy and EBUS-TBNA in October 2008. A diagnosis of lung adenocarcinoma was obtained with TBNA samples from #7 lymph nodes. Bone scans indicated cranial, costal, vertebral, scapular, pelvic and femoral metastases (T4N2M1 stage IV). She received 2 courses of CBDCA+GEM (1000 mg/m^2) and 7 courses of docetaxel (TXTL: 60 mg/m^2) from November 2008 to June 2009, but the effect was minimal.

EML4-ALK fusion gene was suggested immunohistochemically in August 2009 and confirmed by RT-PCR obtained by EBUS-TBNA samples from the primary tumor in September 2009. She was enrolled for the clinical trial from November 2009 with an oral administration of crizotinib 500 mg/day. Dyspnea and cough were alleviated within 2 weeks, and she complained of severe diarrhea, nausea, vomiting, light image persistence and perceived changes of taste. A PET scan one month after the start of the treatment demonstrated complete disappearance of the primary tumor as well as all the metastases except for a bone metastasis to the right 8th rib. A PET scan follow-up 8 months later indicated complete control of primary and metastatic tumors (Fig. 8A and B). CEA declined slowly from 1764 ng/ml to 79 ng/ml 6 months after the start of administration (Fig. 9). The patient had 12 brain metastases from 5 mm^3 to 309 mm^3 in volume and underwent gamma knife irradiation in August 2009, 2 months before the start of ALK inhibitor treatment. The irradiated field still showed little change for 5 months, but small new lesions appeared in the left occipital area 6 months after the start of the trial. Brain metastases grew very slowly, so we have maintained our observation until October 2010.

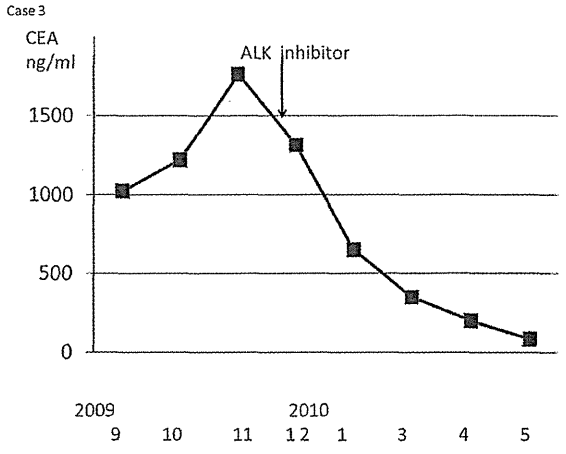

Fig. 9. CEA (■) declined slowly from 1764 ng/ml to 79 ng/ml 6 months after the start of the therapy in case 3.

4. Discussion

Above, we have reported the far-reaching effects of an ALK inhibitor on *EML4-ALK*-positive lung cancer patients. Soon after the administration of crizotinib, almost all metastases to bone and lymph nodes rapidly disappeared, followed by a marked reduction in the level of tumor markers in the sera. These observations clearly support the pivotal role of EML4-ALK oncokinase for the growth/survival of not only primary tumors but of the metastases. Such profound effects were rare among the patients when treated with conventional cytotoxic anticancer drugs.

The three cases which were enrolled for the study had surprisingly similar biological characteristics. They had multiple bone and lymph node metastases at the first medical examination, and were non-smokers at younger ages (48–54) who were resistant to chemotherapy. Adverse effects with crizotinib were also similar among them, including transient diarrhea, nausea, light image persistence, and subjective changes of taste. In addition, their response to ALK inhibitor was similar. Bone and lymph node metastases had disappeared within one month after the initiation of the therapy. The response of the primary tumor in case 2 was relatively slow compared with those of the metastases. The difference between the response of primary tumor and metastases to the ALK inhibitor in this case seems to indicate that the similar subclones of tumor cells in the primary tumors that were highly responsive to ALK inhibitor metastasized to distant organs and may give some explanation for the discrepancy in the time-course between CEA and CA125.

Molecular and immunohistochemical analyses in this cohort were conducted on the basis of the specimens obtained through EBUS-TBNA. Originally, EBUS-TBNA had been proposed useful for the pathological diagnosis of mediastinal involvement (N2 disease) of lung cancer [17–20]. However, we have already reported that EBUS-TBNA is also a versatile way of obtaining histological samples for the molecular analyses of cancer-related genes, such as *EGFR*, p53 et al. [21,22]. For those who have advanced NSCLC, it is often difficult to conduct surgery to obtain specimens from patients. Among such cases, however, EBUS-TBNA can usually be safely carried out to obtain specimens from enlarged mediastinal

lymph nodes or parathracheal tumors. We carried out EBUS-TBNA procedure for the reasons of its advantage in obtaining high quality core samples adequate for this purpose as well as its safety. We do not disregard the importance of TBB for the diagnosis of lung cancer; however, we needed histological samples to examine the immunohistochemistry and FISH for enrolment in a trial of crizotinib. Our experience with the three cases clearly demonstrates the importance and clinical relevance of obtaining such specimens for molecular analyses.

Although the initial effects of crizotinib are substantial in our cases, as well as in those reported by Bang et al. [10,11], such efficacy may not always last long. There was, for instance, development (case 1 and 2) and recurrence (case 3) of brain metastases while favorable control was maintained outside the brain. Given that the primary tumors and lymph node metastases were under control of crizotinib even at the appearance of brain metastases, the tumor cells outside the brain did not lose sensitivity to crizotinib. Relapses in the brain only may indicate either (i) subclones of the tumor acquired both the homing ability to the brain and resistance to crizotinib, or (ii) crizotinib may not penetrate the blood-brain barrier, leading to insufficient concentrations of crizotinib in the brain. It is thus highly important to examine in detail the molecular basis that would account for such acquired resistance to crizotinib, which may be secondary mutations within EML4-ALK itself or mutations/gene amplification of other genes, as demonstrated in the cases of acquired resistance of NSCLC to gefitinib/erlotinib [23–26].

Conflict of interest

None declared.

Acknowledgements

We are grateful to Dr. Yung-Jue Bang and the medical staff of Seoul National University Hospital for their support in the treatment of these patients. We also thank Mr. C.W.P. Reynolds of the Department of International Medical Communications, Tokyo Medical University, for his careful revision of the English of this manuscript.

References

[1] Janku F, Stewart DJ, Kurzrock R. Targeted therapy in non-small-cell lung cancer—Is it becoming a reality? Nat Rev Clin Oncol 2010 Jun 15;7(July (7)):401–14.
[2] Heinrich MC, Owzar K, Corless CL, et al. Correlation of kinase genotype and clinical outcome in the North American intergroup phase III trial of imatinib mesylate for treatment of advanced gastrointestinal stromal tumor: CALGB 150105 study by cancer and leukemia group B and southwest oncology group. J Clin Oncol 2008;26:5360–7.
[3] Mok TS, Wu YL, Yu CJ, et al. Randomized, placebo-controlled, phase II study of sequential erlotinib and chemotherapy as first-line treatment for advanced non-small-cell lung cancer. J Clin Oncol 2009;27:5080–7.
[4] Soda M, Choi YL, Enomoto M, et al. Identification of the transforming EML4-ALK fusion gene in non-small-cell lung cancer. Nature 2007;448:561–6.
[5] Mano H. Non-solid oncogenes in solid tumors: EML4-ALK fusion genes in lung cancer. Cancer Sci 2008;99:2349–55.
[6] Soda M, Takada S, Takeuchi K, et al. A mouse model for EML4-ALK-positive lung cancer. Proc Natl Acad Sci USA 2008;105:19893–7.
[7] Christensen JG, Zou HY, Arango ME, et al. Cytoreductive antitumor activity of PF-2341066, a novel inhibitor of anaplastic lymphoma kinase and c-Met, in experimental models of anaplastic large-cell lymphoma. Mol Cancer Ther 2007;6:3314–22.
[8] Koivunen JP, Mermel C, Zejnullahu K, et al. EML4-ALK fusion gene and efficacy of an ALK kinase inhibitor in lung cancer. Clin Cancer Res 2008;14: 4275–83.
[9] Kwak EL, Camidge DR, Clark J, et al. Clinical activity observed in a phase I dose escalation trial of an oral c-met and ALK inhibitor, PF-02341066. J Clin Oncol 2009;27:15s.
[10] Bang Y, Kwak EL, Shaw AT, et al. Clinical activity of the oral ALK inhibitor PF-02341066 in ALK-positive patients with non-small cell lung cancer (NSCLC). J Clin Oncol 2010;28:18s [suppl; abstr 3].
[11] Kwak EL, Bang YJ, Camidge DR, et al. Anaplastic lymphoma kinase inhibition in non-small-cell lung cancer. N Engl J Med 2010;363:1693–703.
[12] Takeuchi K, Choi YL, Togashi Y, et al. KIF5B-ALK, a novel fusion oncokinase identified by an immunohistochemistry-based diagnostic system for ALK-positive lung cancer. Clin Cancer Res 2009;15:3143–9.
[13] Inamura K, Takeuchi K, Togashi Y, et al. EML4-ALK lung cancers are characterized by rare other mutations, a TTF-1 cell lineage, an acinar histology, and young onset. Mod Pathol 2009;22:508–15.
[14] Shaw AT, Yeap BY, Mino-Kenudson M, et al. Clinical features and outcome of patients with non-small-cell lung cancer who harbor EML4-ALK. J Clin Oncol 2009;27(September (26)):4247–53.
[15] Takahashi T, Snooze M, Kobayashi M, et al. Clinicopathologic features of non-small-cell lung cancer with EML4-ALK fusion gene. Ann Surg Oncol 2010;17(March (3)):889–97.
[16] Nakajima T, Kimura H, Takeuchi K, et al. Treatment of lung cancer with an ALK inhibitor after EML4-ALK fusion gene detection using endobronchial ultrasound-guided transbronchial needle aspiration. J Thorac Oncol 2010;5:2041–3.
[17] Yasufuku K, Chiyo M, Koh E, et al. Endobronchial ultrasound guided transbronchial needle aspiration for staging of lung cancer. Lung Cancer 2005;50:347–54.
[18] Yasufuku K, Chiyo M, Sekine Y, et al. Real-time endobronchial ultrasound-guided transbronchial needle aspiration of mediastinal and hilar lymph nodes. Chest 2004;126:122–8.
[19] Herth FJ, Eberhardt R, Vilmann P, Krasnik M, Ernst A. Real-time endobronchial ultrasound guided transbronchial needle aspiration for sampling mediastinal lymph nodes. Thorax 2006;61:795–8.
[20] Herth FJ, Ernst A, Eberhardt R, Vilmann P, Dienemann H, Krasnik M. Endobronchial ultrasound-guided transbronchial needle aspiration of lymph nodes in the radiologically normal mediastinum. Eur Respir J 2006;28: 910–4.
[21] Nakajima T, Yasufuku K, Suzuki M, et al. Assessment of epidermal growth factor receptor mutation by endobronchial ultrasound-guided transbronchial needle aspiration. Chest 2007;132:597–602.
[22] Mohamed S, Yasufuku K, Nakajima T, et al. Analysis of cell cycle-related proteins in mediastinal lymph nodes of patients with N2-NSCLC obtained by EBUS-TBNA: relevance to chemotherapy response. Thorax 2008;63:642–7.
[23] Kobayashi S, Boggon TJ, Dayaram T, et al. EGFR mutation and resistance of non-small-cell lung cancer to gefitinib. N Engl J Med 2005;352:786–92.
[24] Lu L, Ghose AK, Quail MR, et al. ALK mutants in the kinase domain exhibit altered kinase activity and differential sensitivity to small molecule ALK inhibitors. Biochemistry 2009;48:3600–9.
[25] Gazdar AF. Activating and resistance mutations of *EGFR* in non-small-cell lung cancer: role in clinical response to EGFR tyrosine kinase inhibitors. Oncogene 2009;28:S24–31.
[26] Choi YL, Soda M, Yamashita Y, et al. EML4-ALK mutations in lung cancer that confer resistance to ALK inhibitors. N Engl J Med 2010;363:1734–9.

Carcinogenesis Advance Access published February 29, 2012
Carcinogenesis vol.0 no.0 pp.1–6, 2012
doi:10.1093/carcin/bgs099
Advance Access publication February 10, 2012

Oncogenic *MAP2K1* mutations in human epithelial tumors

Young Lim Choi[1,2], Manabu Soda[1], Toshihide Ueno[1], Toru Hamada[1], Hidenori Haruta[1], Azusa Yamato[1], Kazutaka Fukumura[2], Mizuo Ando[2], Masahito Kawazu[2], Yoshihiro Yamashita[1] and Hiroyuki Mano[1,2,3,*]

[1]Division of Functional Genomics, Jichi Medical University, Tochigi 329-0498, Japan, [2]Department of Medical Genomics, Graduate School of Medicine, University of Tokyo, Tokyo 113-0033, Japan and [3]Core Research for Evolutional Science and Technology, Japan Science and Technology Agency, Saitama 332-0012, Japan

*To whom correspondence should be addressed. Tel: +81 285 58 7449; Fax: +81 285 44 7322;
Email: hmano@jichi.ac.jp

The scirrhous subtype of gastric cancer is a highly infiltrative tumor with a poor outcome. To identify a transforming gene in this intractable disorder, we constructed a retroviral complementary DNA (cDNA) expression library from a cell line (OCUM-1) of scirrhous gastric cancer. A focus formation assay with the library and mouse 3T3 fibroblasts led to the discovery of a transforming cDNA, encoding for MAP2K1 with a glutamine-to-proline substitution at amino acid position 56. Interestingly, treatment with a MAP2K1-specific inhibitor clearly induced cell death of OCUM-1 but not of other two cells lines of scirrhous gastric cancer that do not carry MAP2K1 mutations, revealing the essential role of MAP2K1(Q56P) in the transformation mechanism of OCUM-1 cells. By using a next-generation sequencer, we further conducted deep sequencing of the *MAP2K1* cDNA among 171 human cancer specimens or cell lines, resulting in the identification of one known (D67N) and four novel (R47Q, R49L, I204T and P306H) mutations within MAP2K1. The latter four changes were further shown to confer transforming potential to MAP2K1. In our experiments, a total of six (3.5%) activating mutations in MAP2K1 were thus identified among 172 of specimens or cell lines for human epithelial tumors. Given the addiction of cancer cells to the elevated MAP2K1 activity for proliferation, human cancers with such MAP2K1 mutations are suitable targets for the treatment with MAP2K1 inhibitors.

Introduction

Many growth-promoting or survival signals converge on members of the RAS family of small guanosine triphosphatases, which then activate the mitogen-activated protein kinase (MAPK) signaling pathway, eventually leading to the transcriptional activation or repression of specific genes in the nucleus (1,2). In addition to such canonical RAS-MAPK signaling, RAS-mediated signaling engages in cross talk with various other signaling pathways, such as those mediated by phosphoinositide 3-kinase (3), Janus kinases (4) as well as WNT and β-catenin (5).

Reflecting the central role of the RAS-MAPK cascade in cell proliferation, activated mutants of RAS family members (HRAS, KRAS and NRAS) are among the oncoproteins most frequently detected in human malignancies (2). Discovery of mutations of BRAF in melanoma and colorectal carcinoma further reinforces the substantial contribution of the RAS-MAPK cascade to carcinogenesis (6). The contributions of somatic mutations of other participants in the RAS-MAPK cascade to human carcinogenesis have remained largely unknown, however.

Gastric cancer is the third most prevalent cancer worldwide and is the second leading cause of cancer-related deaths (>1 million deaths per year) (7). Whereas the diagnosis of gastric cancer has become more sensitive and reliable with the implementation of gastrointestinal endoscopy, unresectable gastric cancer remains mostly intractable. Given the promising efficacy of an inhibitor of the anaplastic lymphoma kinase (ALK) in the treatment of non-small cell lung cancer (NSCLC) positive for the EML4-ALK fusion protein (8,9) and of a BRAF inhibitor in the treatment of melanoma positive for BRAF mutations (10), the identification of additional oncogenes on which cancer cells are dependent should provide a basis for the targeting of such genes in the development of anticancer agents with improved efficacy (11).

We have now adopted the OCUM-1 cell line of scirrhous-type gastric cancer to screen for transforming genes. A retroviral complementary DNA (cDNA) expression library was constructed from the OCUM-1 cells and was then used for a focus formation assay with mouse 3T3 fibroblasts. We thereby identified a transforming mutant of MAP2K1 and further showed that OCUM-1 cells are dependent on MAP2K1 activity for growth. Deep sequencing of *MAP2K1* cDNAs among a total of 171 cancer specimens and cell lines further identified known and novel activating mutations of MAP2K1.

Abbreviations: ALK, anaplastic lymphoma kinase; cDNA, complementary DNA; ERK, extracellular signal-regulated kinase; MAPK, mitogen-activated protein kinase; NSCLC, non-small cell lung cancer.

Materials and methods

Cell lines and specimens

Three cell lines of scirrhous-type gastric cancer (OCUM-1, KATOIII and NUGC-4) were obtained from the Japanese Collection of Research Bioresources (Osaka, Japan), and HEK293 and 3T3 cell lines were obtained from American Type Culture Collection (Manassas, VA). These cells were maintained in Dulbecco's modified Eagle's medium-F12 (Invitrogen, Carlsbad, CA) supplemented with 10% fetal bovine serum and 2 mM L-glutamine (both from Invitrogen). Where indicated, cells were incubated with 20 nM of the MAP2K1 inhibitor AZD6244 (Selleckchem, Houston, TX). Total RNA was extracted from cell lines and cancer specimens with an RNeasy Mini Kit (Qiagen, Valencia, CA) and was subjected to reverse transcription with an oligo(deoxythymidine) primer. Written informed consent was obtained from the subjects who provided cancer specimens, and the study was approved by the human ethics committee of Jichi Medical University.

Focus formation assay

Recombinant ecotropic retroviruses for expression of OCUM-1 cell cDNAs were constructed as described previously (8). Mouse 3T3 cells were infected with the retroviral library at a multiplicity of infection of 0.1 infectious particle per cell, and the cells were then cultured for 2–3 weeks in Dulbecco's modified Eagle's medium-F12 medium supplemented with 5% calf serum (Invitrogen). Genomic DNA was extracted from transformed foci and was subjected to PCR with 5′-PCR primer IIA (Clontech, Mountain View, CA) in order to rescue retrovirus inserts. The nucleotide sequence of rescued cDNAs was determined with a Sanger sequencer.

Functional assay of MAP2K1

The cDNAs for wild-type or mutant forms of MAP2K1 were inserted into the retroviral plasmid pMXS (12), and the modified plasmids were then used to generate recombinant ecotropic retroviruses. Each virus was used to infect 3T3 cells, which were subsequently subjected to a focus formation assay as well as a tumorigenicity assay with nude mice, the latter of which was approved by the institutional review board for animal experiments in Jichi Medical University. The viral plasmids were also used to transfect HEK293 cells by the calcium phosphate method, and the transfected cells were subsequently subjected to immunoblot analysis with antibodies to phosphorylated or total forms of extracellular signal-regulated kinase (ERK) (both from Cell Signaling Technology).

Multiplex deep sequencing of MAP2K1 cDNAs

The entire open reading frame of *MAP2K1* cDNA was amplified by PCR with the primers 5′-AGCGGATCCCCCGGGTCCAAAATGCCC-3′ and 5′-CTTCTCGAGCACTTAGACGCCAGCAGC-3′ from total cDNAs of 171 cancer specimens or cell lines, and the amplification products were fragmented and then subjected to deep sequencing with a Genome Analyzer IIx (GAIIx; Illumina, San Diego, CA) for 76 bases from both ends of each fragment with the paired-end sequencing option. We modified the paired-end adaptors (Illumina) for a multiplex reaction so that an 'N_1N_2' or 'X_2X_1' doublet was added to the 5′ or 3′ end, respectively, of cDNA fragments (N_1 and N_2 are any bases

but are complementary to X_1 and X_2, respectively). Fragmented cDNAs of each sample were ligated to our custom paired-end adaptors, and the 'two-base tag' of N_1N_2/X_1X_2 sequences was used to assign read data to the original sample. Given the availability of 16 independent two-base codes, a single lane of the Illumina flow cell can simultaneously run up to 16 samples. The *MAP2K1* mutations identified in the GAIIx data sets were further confirmed by genomic PCR analysis of the corresponding regions of the gene followed by Sanger sequencing.

Results

Identification of MAP2K1(Q56P) in OCUM-1 cells

The scirrhous subtype of gastric carcinoma (diffusely infiltrating carcinoma or Borrmann type IV) is a highly infiltrating poorly differentiated gastric cancer with a 5 year survival rate of only 11.3% (13). Despite the discovery of germ-line mutations in *CDH1* associated with familial diffuse-type gastric cancer (14), such mutations are present at only a relatively low frequency among sporadic cases, and little is known of the driver mutations for this intractable disorder. To identify transforming genes in scirrhous gastric cancer, we constructed a cDNA expression library from a cell line (OCUM-1) established from an individual with this condition. A focus formation assay performed with 3T3 cells infected with the retroviral library resulted in the identification of a dozen transformed foci. Recovery and nucleotide sequencing of insert cDNAs from such foci revealed that one of the cDNAs was derived from human *MAP2K1* with a nucleotide substitution of A-to-C at position 642 of the cDNA (GenBank accession number, NM_002755). Sequencing of this position in OCUM-1 genomic DNA confirmed the presence of this substitution, which results in replacement of a glutamine at amino acid position 56 with proline (Supplementary Figure 1 is available at *Carcinogenesis* Online). MAP2K1, also known as MEK1, functions immediately upstream of MAPK in the MAPK signaling pathway.

Transforming ability of MAP2K1(Q56P)

The MAP2K1(Q56P) mutation was first detected by *in vitro* screening to identify activated components of the RAS-MAPK signaling cascade in rat fibroblasts (15), and it was later identified in a human lung cancer cell line (16). We confirmed the transforming ability of MAP2K1(Q56P) by using a focus formation assay with mouse 3T3 fibroblasts (Figure 1A) and a tumorigenicity assay with nude mice (Figure 1B). Furthermore, such potential of MAP2K1(Q56P) was canceled by eliminating its enzymatic activity (through a replacement of lysine-97 in the adenosine triphosphate-binding pocket to a methionine) or by incubation with a selective MAP2K1/2 inhibitor, AZD6244 (17).

Although the Q56P mutation was previously shown to confer an ~10-fold increase in the enzymatic activity of MAP2K1 (15), little has been known of the dependence of cancer cells on MAP2K1(Q56P) for viability. To address this issue, we compared the effect of AZD6244 on OCUM-1 cells with that on two other cell lines of human scirrhous-type gastric cancer, KATOIII and NUGC-4. Sanger sequencing of genomic DNA from the latter two cell lines confirmed the absence of mutations that could give rise to the Q56P substitution (data not shown). Treatment with AZD6244 inhibited the proliferation of OCUM-1 cells but not that of KATOIII or NUGC-4 cells (Figure 2A), showing that MAP2K1(Q56P) is a suitable target for drug development. Furthermore, in OCUM-1 cells, phosphorylation of ERK1/2 was substantially decreased upon the AZD6244 treatment (Figure 2B) but such effect was less prominent in the other cell lines.

Multiplex deep sequencing of MAP2K1 cDNAs

Given the dependence of OCUM-1 cells on MAP2K1(Q56P) for survival, we next searched for transforming *MAP2K1* mutations in other epithelial tumors. It should be noted, however, that epithelial tumors are frequently contaminated with inflammatory cells and fibrous or necrotic tissue (especially in the case of infiltrative scirrhous-type gastric cancer), which makes it difficult to determine the presence or absence of *MAP2K1* mutations with the use of conventional Sanger sequencing. We therefore chose a deep sequencing approach with the use of a next-generation sequencer. To facilitate simultaneous sequencing of multiple samples, we added two-base tags to the

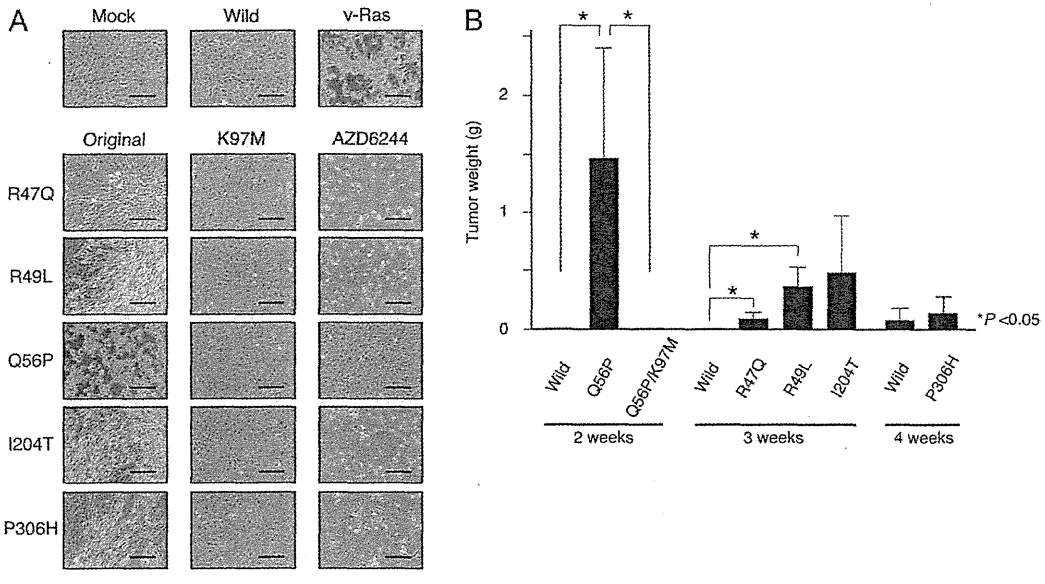

Fig. 1. Transforming potential of MAP2K1 mutants. (**A**) Recombinant retroviruses encoding MAP2K1 (Wild), the indicated MAP2K1 mutants or v-Ras or the corresponding empty virus (Mock), were used to infect 3T3 cells, which were then cultured for 13 days and photographed. Scale bars, 400 μm. The kinase-dead form (K97M) of each mutant was similarly analyzed. In addition to the cells expressing original mutants, the same set of cells was separately treated with 400 nM of AZD6244 for 13 days. (**B**) Mouse 3T3 cells expressing wild-type MAP2K1, Q56P or its kinase-dead form (Q56P/K97M) were injected subcutaneously into the shoulder of nu/nu mice, and tumor weight was examined after 2 weeks. Likewise, tumor weight for the cells expressing wild MAP2K1, R47Q, R49L or I204T mutant was examined after 3 weeks and that for cells expressing wild MAP2K1 or the P306H mutant was examined after 4 weeks. Data are means ± SD of values from four injection sites. The difference in tumor size is evaluated by Student's *t*-test.

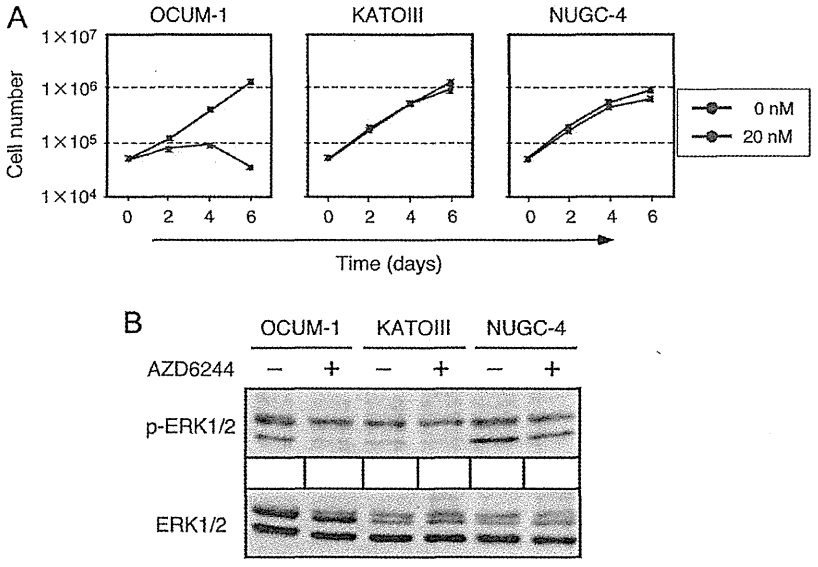

Fig. 2. MAP2K1(Q56P)-dependent growth of OCUM-1 cells. (**A**) OCUM-1, KATOIII and NUGC-4 cells were cultured in the absence or presence of AZD6244 (20 nM), and cell number was determined at the indicated times. Data are means ± SD from three separate experiments. (**B**) Total cell lysates were obtained from each cell line treated with (+) or without (–) 400 nM of AZD6244 for 24 h and probed with antibodies to phosphorylated (p-) or total forms of ERK1/2.

paired-end adaptors used for PCR amplification of fragmented *MAP2K1* cDNAs to be analyzed by a GAIIx sequencer (Figure 3A). The first two bases in each GAIIx read sequence thus correspond to the tag. The diversity of the tag sequences allows a total of 16 independent samples to be analyzed together in a single lane of an Illumina flow cell.

We amplified the entire coding region of *MAP2K1* cDNA from a total of 171 cell lines or clinical specimens of human epithelial cancer, including 26 samples of esophageal cancer (14 cell lines and 12 specimens), 88 samples of gastric cancer (2 cell lines, 46 specimens with a pathological classification of poorly differentiated cell morphology and 40 specimens with well-differentiated cell morphology), 13 samples of breast cancer (2 cell lines and 11 specimens) and 44 specimens of colon cancer. The resulting cDNAs were then subjected to multiplex deep sequencing with four to six different samples (with different tags) run in the same lanes.

A BLAST search of non-synonymous substitutions in the *MAP2K1* sequence revealed an additional five amino acid changes (2.9%) in our 171 samples: I204T in a specimen of poorly differentiated gastric cancer (scirrhous-type), R47Q in a specimen of breast cancer and R49L, D67N and P306H in different specimens of colon cancer (Figure 3B; Supplementary Table 1 is available at *Carcinogenesis* Online). The proportion of mutant reads within the total coverage varied substantially among specimens. For instance, *MAP2K1* reads containing a G-to-A substitution at nucleotide position 140 for the R47Q change in breast cancer occupied ~94% of total reads at this position, suggesting a loss of heterozygosity at the *MAP2K1* locus. In contrast, the reads containing a T-to-C substitution for the I204T change occupied only 7.9% of the total reads from the specimen of scirrhous-type gastric cancer, confirming the low percentage of tumor cells in a given specimen for this highly infiltrative cancer.

We next examined whether these point mutations were somatic alterations by sequencing genomic DNA for the corresponding regions prepared from the tumor as well as paired non-tumor tissue. Unfortunately, an extra specimen for the breast cancer patient (MMK5) was not available, and so we were not able to confirm the genomic change responsible for the R47Q mutation. For this patient, however, the G-to-A change was readily confirmed in cDNA sequencing by the Sanger method (data not shown). For the other four mutations, we did confirm cancer-specific sequence alterations in genomic DNA (Figure 3C). We thus identified a total of six amino acid substitutions in MAP2K1, two (Q56P and D67N) of which had been described previously and had their transforming ability confirmed (16,18), but the remaining four were novel.

Transforming ability of mutant MAP2K1 proteins

To assess the transforming potential of the novel MAP2K1 mutations, we constructed recombinant retroviruses encoding each mutant in order to infect mouse 3T3 fibroblasts. Incubation of the cells for 13 days led to the formation of multiple transformed foci with each mutant but not with wild-type MAP2K1 (Figure 1A). As in the case for the Q56P mutant, no transformed foci were detected for the kinase-dead forms (K97M) or with the incubation with AZD6244. As demonstrated in Figure 1A, a sustained treatment with the compound induced marked cell death among the 3T3 cells except for those expressing the Q56P mutant. Furthermore, it should be noted that the number of transformed foci expressing the R47Q or P306H mutant was substantially fewer than that of cells expressing the other mutants.

Such 3T3 cells were also injected into the shoulder of nu/nu mice (Figure 1B). At 3 weeks after the injection, all of the R47Q, R49L and I204T mutants but not wild-type MAP2K1 or the P306H mutant, generated palpable tumors at every injection site. These data further confirmed the transforming potential of the R47Q, R49L and I204T mutants in addition to Q56P. At 4 weeks after the 3T3 injection, we could identify subcutaneous tumors for the P306H, but the cells expressing wild-type MAP2K1 generated small tumors at several sites as well. Therefore, the transforming potential for MAP2K1(P306H) may be modest.

To examine the effect of the MAP2K1 mutants on the activation status of the downstream kinases ERK1/2, we introduced MAP2K1 or its mutants into HEK293 cells and evaluated the phosphorylation level of ERK1/2 by immunoblot analysis (Figure 3D). Expression of wild-type MAP2K1 resulted in only a small increase in the level of phosphorylation (activation) of ERK1/2. In contrast, MAP2K1(Q56P) induced a marked increase in ERK1/2 activity, whereas a kinase-dead form of this mutant had largely lost this ability, suggesting that MAP2K1(Q56P) activates ERK1/2 in a manner dependent on its enzymatic activity. All of the other mutants tested (R47Q, R49L, I204T and P306H) also markedly increased the level of ERK1/2 phosphorylation, further confirming their activating potential.

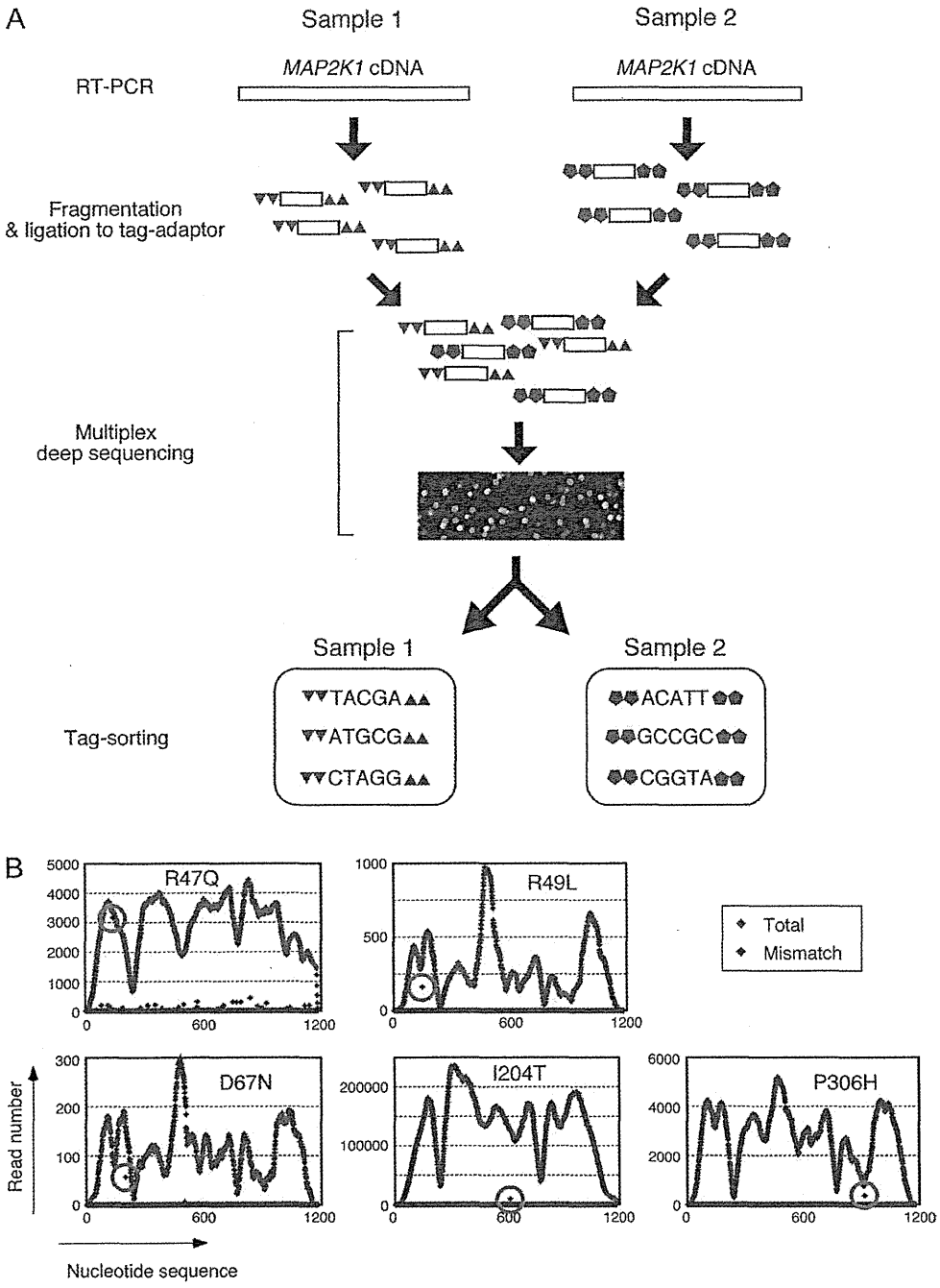

Fig. 3. Multiplex deep sequencing of *MAP2K1* cDNAs. (**A**) *MAP2K1* cDNA was synthesized from 171 cell lines or clinical specimens, fragmented and ligated to sample-specific two-base-tagged adaptors. The cDNA fragments with different two-base tags were mixed and subjected to deep sequencing in the same lane of an Illumina flow cell. The resultant read sequences were sorted, with the two-base tags used as an identification number for each sample. (**B**) *MAP2K1* cDNAs obtained from five cancer specimens harboring the R47Q, R49L, D67N, I204T or P306H mutations were sequenced with the GAIIx system. The numbers for total read coverage (Total) and mismatched reads (Mismatch) are shown at each position of the cDNAs with blue and red diamonds, respectively. The position for mismatched reads for each *MAP2K1* mutation is indicated by a green circle. (**C**) Genomic DNA corresponding to R49, D67, I204 or P306 positions of MAP2K1 was amplified by PCR from tumor and paired normal tissue specimens and was then subjected to Sanger sequencing. Mutated bases are shown in red letters. The PCR product for the tumor harboring the I204T mutation was cloned into a plasmid vector before Sanger sequencing. (**D**) Expression vectors for MAP2K1 (Wild), MAP2K1(Q56P), the kinase-dead mutant MAP2K1(Q56P/K97M), MAP2K1(R47Q), MAP2K1(R49L), MAP2K1(I204T) or MAP2K1(P306H) or the corresponding empty vector (–), were introduced into HEK293 cells. Lysates of the transfected cells were subjected to immunoblot analysis with antibodies to phosphorylated (p-) or total forms of ERK1/2.

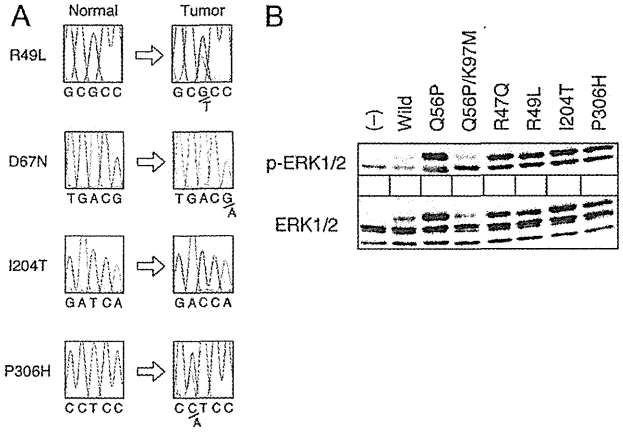

Fig. 3. *continued.*

Discussion

We have identified the Q56P mutant of MAP2K1 in a cell line of scirrhous-type gastric cancer and have shown that these cancer cells are dependent on the mutated MAP2K1 for growth. Furthermore, deep sequencing of *MAP2K1* cDNAs derived from 171 cancer cell lines or clinical specimens revealed one known and four novel mutations of MAP2K1, all of which possess transforming potential. A total of six (3.5%) distinct activating mutations were thus discovered for MAP2K1 in our cohort of 172 cell lines and clinical specimens (Figure 4).

In addition to MAP2K1 mutations identified in individuals with congenital cardiofaciocutaneous syndrome (19), MAP2K1 mutations have been detected in various cancers, albeit infrequently (20). The D67N substitution was discovered in 1 of 15 ovarian cancer cell lines (18). On the other hand, two cases of NSCLC harboring a somatic K57N mutation of MAP2K1 were detected among 207 primary tumor specimens, whereas the Q56P change was identified in 1 of 85 NSCLC cell lines (16). Furthermore, two cases of colorectal cancer harboring a somatic amino acid change (R201H or E203K) of MAP2K1 were detected by screening of 55 cases, but none of 38 cases of breast cancer was found to be associated with a MAP2K1 mutation (21); the same study also found MAP2K1(Y134C) in one cancer cell line. Whereas the Q56P, K57N and D67N substitutions are known to activate MAP2K1, it remains unclear whether these other amino acid changes affect MAP2K1 activity. These previous data, together with our present results, thus suggest that MAP2K1 is infrequently activated by point mutations in various epithelial tumors.

Interestingly, the transforming potential of the MAP2K1 mutants did not correlate always with the phosphorylation level of their downstream targets ERK1/2. While all of R47Q, R49L, Q56P, I204T and P306H mutations similarly induced phosphorylation of ERK1/2 in HEK293 cells (Figure 3D), their transforming potential as judged by 3T3 cells substantially differs (Figure 1). Furthermore, mouse 3T3 cells have a high level of ERK1/2 phosphorylation, and introduction of MAP2K1 mutants only slightly affect the phosphorylation level (data not shown). These data may imply that MAP2K1-dependent transformation of 3T3 cells is, at least, partially mediated through ERK1/2-independent pathways as demonstrated previously (22) or is cell context-dependent.

Known and novel MAP2K1 mutations appear to cluster in two hotspots (Figure 4): a hinge region (R47, R49, Q56, K57 and D67) between the coiled-coil and catalytic domains and the activation loop of the kinase domain (R201, E203 and I204). Amino acid substitutions in the activation loop frequently increase enzymatic activity in a wide variety of protein kinases (23). With regard to the hinge region, artificial truncation of the coiled-coil domain was shown previously to result in constitutive activation of MAP2K1 (24). It is thus likely that

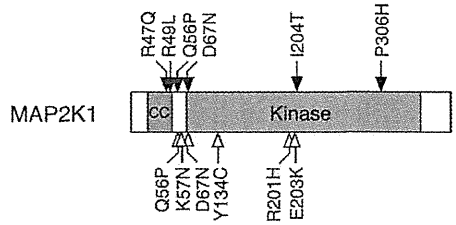

Fig. 4. Schematic representation of the protein structure of MAP2K1 showing amino acid substitutions identified in the present study (closed arrows) and in previous studies (open arrows). CC, coiled-coil domain.

the coiled-coil domain of MAP2K1 negatively regulates enzymatic activity and that mutations that affect the proper structure or function of the coiled-coil domain may release the enzymatic activity of MAP2K1 from such inhibition.

In our study, we took advantage of multiplex deep sequencing to screen for mutations of *MAP2K1* cDNA in a sensitive manner, allowing interrogation of the target cDNA at a high level of coverage among hundreds of samples. Such deep sequencing is likely to be especially important for analysis of specimens of infiltrative tumors or of tumors with large amounts of necrotic tissue, as shown by the detection of the I204T mutation as a low proportion of reads for a specimen of scirrhous-type gastric cancer. Likewise, from pleural effusion of a patient with NSCLC positive for EML4-ALK, we detected a small fraction of tumor cells with acquired mutations responsible for resistance to an ALK inhibitor (25). Such an approach should prove useful for the detection of *MAP2K1* mutations in other types of cancer, and it potentially constitutes a relatively simple, yet highly sensitive, approach to the screening of any target gene or cDNA for nucleotide changes among hundreds of clinical specimens.

Supplementary material

Supplementary Table 1 and Figure 1 can be found at http://carcin.oxfordjournals.org/.

Funding

This study was supported in part by grants for Research on Human Genome Tailor-made and for Third-Term Comprehensive Control Research for Cancer from the Ministry of Health, Labor, and Welfare of Japan, by Grants-in-Aid for Scientific Research (B) and for Young Scientists (A) from the Ministry of Education, Culture, Sports, Science, and Technology of Japan and by grants from the Japan Society

for the Promotion of Science, from Takeda Science Foundation, from the Naito Foundation, from Sankyo Foundation of Life Science, from The Sagawa Foundation for Promotion of Cancer Research, from the Yasuda Medical Foundation, from the Mitsubishi Foundation, and from Kobayashi Foundation for Cancer Research.

Conflict of Interest Statement: None declared.

References

1. Sebolt-Leopold,J.S. *et al.* (2004) Targeting the mitogen-activated protein kinase cascade to treat cancer. *Nat. Rev. Cancer*, **4**, 937–947.
2. Karnoub,A.E. *et al.* (2008) Ras oncogenes: split personalities. *Nat. Rev. Mol. Cell Biol.*, **9**, 517–531.
3. Downward,J. (2008) Targeting RAS and PI3K in lung cancer. *Nat. Med.*, **14**, 1315–1316.
4. Rane,S.G. *et al.* (2000) Janus kinases: components of multiple signaling pathways. *Oncogene*, **19**, 5662–5679.
5. Ishitani,T. *et al.* (1999) The TAK1-NLK-MAPK-related pathway antagonizes signalling between beta-catenin and transcription factor TCF. *Nature*, **399**, 798–802.
6. Davies,H. *et al.* (2002) Mutations of the BRAF gene in human cancer. *Nature*, **417**, 949–954.
7. American Cancer Society. (2008) *Global Cancer Facts and Figures 2007.* http://www.cancer.org/docroot/STT/content/STT_1x_Cancer_Facts_and_Figures_2008.asp?from=fast (22 February 2012, date last accessed).
8. Soda,M. *et al.* (2007) Identification of the transforming *EML4-ALK* fusion gene in non-small-cell lung cancer. *Nature*, **448**, 561–566.
9. Kwak,E.L. *et al.* (2010) Anaplastic lymphoma kinase inhibition in non-small-cell lung cancer. *N. Engl. J. Med.*, **363**, 1693–1703.
10. Flaherty,K.T. *et al.* (2010) Inhibition of mutated, activated BRAF in metastatic melanoma. *N. Engl. J. Med.*, **363**, 809–819.
11. Weinstein,I.B. *et al.* (2006) Mechanisms of disease: oncogene addiction–a rationale for molecular targeting in cancer therapy. *Nat. Clin. Pract. Oncol.*, **3**, 448–457.
12. Onishi,M. *et al.* (1996) Applications of retrovirus-mediated expression cloning. *Exp. Hematol.*, **24**, 324–329.
13. Chen,C.Y. *et al.* (2002) Peritoneal carcinomatosis and lymph node metastasis are prognostic indicators in patients with Borrmann type IV gastric carcinoma. *Hepatogastroenterology*, **49**, 874–877.
14. Guilford,P. *et al.* (1998) E-cadherin germline mutations in familial gastric cancer. *Nature*, **392**, 402–405.
15. Bottorff,D. *et al.* (1995) RAS signalling is abnormal in a c-raf1 MEK1 double mutant. *Mol. Cell. Biol.*, **15**, 5113–5122.
16. Marks,J.L. *et al.* (2008) Novel MEK1 mutation identified by mutational analysis of epidermal growth factor receptor signaling pathway genes in lung adenocarcinoma. *Cancer Res.*, **68**, 5524–5528.
17. Yeh,T.C. *et al.* (2007) Biological characterization of ARRY-142886 (AZD6244), a potent, highly selective mitogen-activated protein kinase kinase 1/2 inhibitor. *Clin. Cancer Res.*, **13**, 1576–1583.
18. Estep,A.L. *et al.* (2007) Mutation analysis of BRAF, MEK1 and MEK2 in 15 ovarian cancer cell lines: implications for therapy. *PLoS ONE*, **2**, e1279.
19. Dentici,M.L. *et al.* (2009) Spectrum of MEK1 and MEK2 gene mutations in cardio-facio-cutaneous syndrome and genotype-phenotype correlations. *Eur. J. Hum. Genet.*, **17**, 733–740.
20. Pao,W. *et al.* (2011) New driver mutations in non-small-cell lung cancer. *Lancet Oncol*, **12**, 175–180.
21. Bentivegna,S. *et al.* (2008) Rapid identification of somatic mutations in colorectal and breast cancer tissues using mismatch repair detection (MRD). *Hum. Mutat.*, **29**, 441–450.
22. Tong,C. *et al.* (2003) Effects of MEK inhibitor U0126 on meiotic progression in mouse oocytes: microtuble organization, asymmetric division and metaphase II arrest. *Cell Res.*, **13**, 375–383.
23. Yamaguchi,H. *et al.* (1996) Structural basis for activation of human lymphocyte kinase Lck upon tyrosine phosphorylation. *Nature*, **384**, 484–489.
24. Mansour,S.J. *et al.* (1994) Transformation of mammalian cells by constitutively active MAP kinase kinase. *Science*, **265**, 966–970.
25. Choi,Y.L. *et al.* (2010) EML4-ALK mutations in lung cancer that confer resistance to ALK inhibitors. *N. Engl. J. Med.*, **363**, 1734–1739.

Received August 5, 2011; revised January 23, 2012; accepted February 6, 2012

OPEN ACCESS Freely available online

PLoS one

Ex Vivo Expansion of Human CD8$^+$ T Cells Using Autologous CD4$^+$ T Cell Help

Marcus O. Butler[1,2,3], Osamu Imataki[1,2,3], Yoshihiro Yamashita[4], Makito Tanaka[1,2,3], Sascha Ansén[1,2,3], Alla Berezovskaya[1], Genita Metzler[1], Matthew I. Milstein[1], Mary M. Mooney[1], Andrew P. Murray[1], Hiroyuki Mano[4,5], Lee M. Nadler[1,2,3], Naoto Hirano[1,2,3,6,7]*

1 Department of Medical Oncology, Dana-Farber Cancer Institute, Massachusetts, United States of America, **2** Department of Medicine, Brigham and Women's Hospital, Massachusetts, United States of America, **3** Department of Medicine, Harvard Medical School, Boston, Massachusetts, United States of America, **4** Division of Functional Genomics, Jichi Medical University, Tochigi, Japan, **5** Department of Medical Genomics, University of Tokyo, Tokyo, Japan, **6** Immune Therapy Program, Campbell Family Institute for Breast Cancer Research, Campbell Family Cancer Research, Ontario Cancer Institute, Toronto, Ontario, Canada, **7** Department of Immunology, University of Toronto, Toronto, Ontario, Canada

Abstract

Background: Using *in vivo* mouse models, the mechanisms of CD4$^+$ T cell help have been intensively investigated. However, a mechanistic analysis of human CD4$^+$ T cell help is largely lacking. Our goal was to elucidate the mechanisms of human CD4$^+$ T cell help of CD8$^+$ T cell proliferation using a novel *in vitro* model .

Methods/Principal Findings: We developed a genetically engineered novel human cell-based artificial APC, aAPC/mOKT3, which expresses a membranous form of the anti-CD3 monoclonal antibody OKT3 as well as other immune accessory molecules. Without requiring the addition of allogeneic feeder cells, aAPC/mOKT3 enabled the expansion of both peripheral and tumor-infiltrating T cells, regardless of HLA-restriction. Stimulation with aAPC/mOKT3 did not expand Foxp3$^+$ regulatory T cells, and expanded tumor infiltrating lymphocytes predominantly secreted Th1-type cytokines, interferon-γ and IL-2. In this aAPC-based system, the presence of autologous CD4$^+$ T cells was associated with significantly improved CD8$^+$ T cell expansion *in vitro*. The CD4$^+$ T cell derived cytokines IL-2 and IL-21 were necessary but not sufficient for this effect. However, CD4$^+$ T cell help of CD8$^+$ T cell proliferation was partially recapitulated by both adding IL-2/IL-21 and by upregulation of IL-21 receptor on CD8$^+$ T cells.

Conclusions: We have developed an *in vitro* model that advances our understanding of the immunobiology of human CD4$^+$ T cell help of CD8$^+$ T cells. Our data suggests that human CD4$^+$ T cell help can be leveraged to expand CD8$^+$ T cells *in vitro*.

Citation: Butler MO, Imataki O, Yamashita Y, Tanaka M, Ansén S, et al. (2012) Ex Vivo Expansion of Human CD8$^+$ T Cells Using Autologous CD4$^+$ T Cell Help. PLoS ONE 7(1): e30229. doi:10.1371/journal.pone.0030229

Editor: Derya Unutmaz, New York University, United States of America

Received April 7, 2011; **Accepted** December 13, 2011; **Published** January 12, 2012

Funding: This work was supported by the Madeleine Franchi Ovarian Research Fund (MOB), Dunkin Donuts Rising Stars Awards (MOB and NH), a grant from the Cancer Research Institute (LMN), NIH grant K22 CA129240 (NH), NIH grant R01 CA148673 (NH), and the American Society of Hematology Scholar Award (NH). The funders had no role in study design, data collection and analysis, decision to publish, or preparation of the manuscript.

Competing Interests: MOB, LMN and NH have filed a patent application related to aAPC/A2. The patent application number is 10/850,294 and is entitled, "Modified Antigen-Presenting Cells." The authors confirm that this application does not alter their adherence to all PLoS ONE policies on the sharing of data and materials.

* E-mail: nhirano@uhnres.utoronto.ca

Introduction

It is now well accepted that neoplastic cells are immunogenic and that tumors develop in the context of immune recognition by the host [1,2]. Tumor-associated antigens that serve as immune targets include cell lineage differentiation antigens, cancer-testes antigens, and neoantigens produced by mutations in the cancer cell's unstable genome. Mutational events can give rise to multiple immunogenic MHC class I and II restricted, non-self epitopes capable of inducing strong immune responses to the tumor [3,4]. In several maligancies, anti-tumor T cell responses, with infiltration of tumors by CD8$^+$ T lymphocytes and local production of interferon-γ and IL-2, have been associated with improved clinical prognosis [5–8].

Counter regulatory immune responses, however, also develop in the cancer-bearing host. Tumors subvert the immune response by secreting chemotactic factors that recruit immune suppressive elements, thereby inhibiting the function of anti-tumor effectors [9]. Tumor infiltration by T regulatory (Treg) cells has been correlated with inferior clinical outcomes in several tumors [10,11]. These findings have led to the proposal that immune recognition of cancer involves the balancing of opposing forces: anti-tumor effectors vs. pro-tumor regulatory elements [10,12,13]. In fact, a high ratio of Treg cells to CD8$^+$ T cells within the tumor microenvironment has been associated with poorer survival [14,15].

Adoptive T cell therapy is a promising treatment modality designed to amplify the anti-tumor immune response. Anti-tumor effectors are expanded *in vitro*, away from the pro-tumor milieu of the cancer bearing host, and then reinfused as a cellular therapy [16–21]. Successful approaches showing clinical activity include adoptive transfer of tumor antigen-specific T cell lines or clones

that have been derived from the peripheral blood. Specificity can be achieved by stimulating antigen-specific precursor T cells or through genetic modification of expanded bulk T cells to express cloned or chimeric T cell receptor (TCR) genes [22–26]. Alternatively, the nascent, endogenous immune effector response to the tumor can be amplified by expanding tumor-infiltrating lymphocytes (TIL) *in vitro*. Adoptive cell transfer of *in vitro* activated TIL has achieved major clinical responses when patients first undergo lymphodepletion and are then given high dose IL-2 after adoptive transfer [17,27]. Lymphodepletion augments the persistence and function of transferred TIL not only by reducing or temporarily eliminating Treg cells, but also by reducing cytokine sinks that results in the accumulation of homeostatic cytokines such as IL-7 and IL-15 [28,29].

The optimal method for generating clinically effective T cell grafts *in vitro* has yet to be established [21,30]. In order to achieve massive numerical expansion of T cells, current methods necessitate the use of soluble monoclonal antibodies (mAb), allogeneic feeder PBMC, EBV transformed lymphoblastoid cell lines, and/or undefined culture supernatants. Consequently, these requirements present formidable challenges and costs that prevent the widespread clinical application of this therapy. While adoptive transfer of anti-tumor $CD4^+$ T cells can be efficacious, expansion of anti-tumor $CD8^+$ T cells is also an important goal, particularly in light of the association between their persistence and clinical responses [18,31–33].

Insights into requirements for augmenting the expansion of both $CD4^+$ and $CD8^+$ T cells will help further improve methods to generate T cell grafts for adoptive therapy. $CD4^+$ T cells help generate effective immune responses by sustaining $CD8^+$ T cell proliferation, preventing exhaustion, and establishing long-lived functional memory [34]. In mouse models, common γ-chain receptor cytokine and CD40 signaling can mediate $CD4^+$ T cell help [34–44]. In clinical studies, $CD4^+$ T cells have also been implicated in promoting the persistence and anti-tumor activity of antigen-specific $CD8^+$ T cells in patients [45,46]. However, the mechanisms of human $CD4^+$ T cell help are less well understood. To conduct a mechanistic analysis of human $CD4^+$ T cell help, we developed a novel, human cell-based aAPC, aAPC/mOKT3, which induces both $CD4^+$ and $CD8^+$ T cell expansion without allogeneic feeder cells. The removal of allogeneic feeder cells from our T cell culture system enabled us to precisely isolate molecules mediating help of $CD8^+$ T cell expansion that are expressed or secreted by human $CD4^+$ T cells.

Results

K562-based aAPC expressing membranous OKT3 induces $CD3^+$ T cell expansion

We and others have previously reported the generation of aAPC derived from the human erythroleukemia cell line K562 [47–51]. K562 serves as an excellent platform for generating aAPC since it expresses no HLA class I or II molecules, but highly expresses adhesion molecules such as CD54 and CD58. Using K562, we developed a novel aAPC, aAPC/mOKT3, capable of expanding $CD3^+$ T cells regardless of HLA subtype (Figure 1A, Figure S1). This aAPC was engineered to express a membranous form of the anti-CD3 mAb, OKT3, on its cell surface, thus obviating the need for adding soluble mAb to T cell cultures or loading it onto aAPC as described elsewhere [51,52]. aAPC/mOKT3 also ectopically expresses immunostimulatory molecules CD80 and CD83. We and others have shown that CD83 delivers a CD80 dependent signal that promotes lymphocyte longevity [47,53,54].

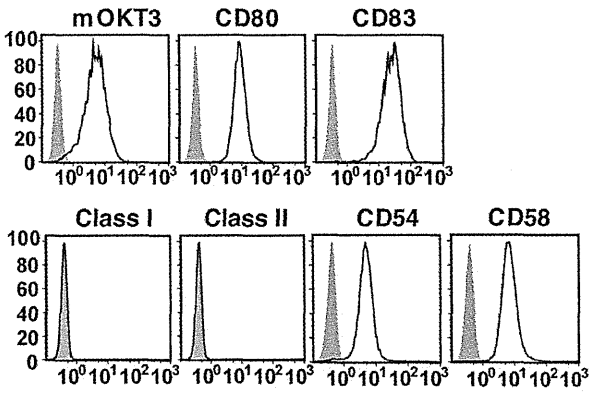

Figure 1. Generation of aAPC/mOKT3. Surface expression of a transduced membranous form of anti-CD3 mAb, and transduced CD80, CD83, and endogenous HLA class I, class II, CD54, and CD58 on aAPC/mOKT3 is shown. A membranous form of anti-CD3 mAb on aAPC/mOKT3 (open) and wild type K562 (shaded) was stained using goat anti-mouse IgG (H+L). Other surface molecules were stained with each specific mAb (open) and isotype control (shaded) and analyzed by flow cytometry. Note the lack of endogenous expression of HLA class I and II on aAPC/mOKT3.
doi:10.1371/journal.pone.0030229.g001

Stimulation of $CD3^+$ T cells with aAPC/mOKT3 induces robust $CD8^+$ T cell expansion

Peripheral $CD3^+$ T cells expanded with aAPC/mOKT3 were phenotypically characterized after 28 days in culture (Figure 2). While the number of both $CD4^+$ and $CD8^+$ T cells increased, $CD8^+$ T cells expanded substantially better than $CD4^+$ T cells, and therefore dominated cultures from every donor tested (Figure 2A). This is in contrast to other pan T cell expansion systems such as anti-CD3/CD28 mAb-coated beads, which invariably favor the expansion $CD4^+$ T cells over $CD8^+$ T cells [55] (Figure 2B). Similar fold expansion of $CD3^+$ T cells was obtained with the aAPC/mOKT3-based and antibody-coated bead-based expansion systems. T cells expanded using aAPC/mOKT3 displayed a central memory~effector memory phenotype ($CD45RA^-$ $CD54RO^+$ $CD62L^{+/-}$) and retained expression of receptors for IL-2, IL-7, and IL-21 (Figure 2C). CD40 ligand was highly expressed by $CD4^+$ T cells but not $CD8^+$ T cells. Importantly, expanded $CD4^+$ $CD25^+$ T cells did not express Foxp3, indicating that immunoinhibitory Treg cells did not proliferate well (Figure 2D).

aAPC/mOKT3 induces unbiased $CD3^+$ T cell expansion, preserving the repertoire for viral and tumor-associated antigens

In order to evaluate whether stimulation with aAPC/mOKT3 induced broad expansion of $CD3^+$ T cells, TCR Vβ repertoire analysis was performed. No obvious skewing in the TCR Vβ usage of both $CD4^+$ and $CD8^+$ T cell populations was revealed, supporting "unbiased" T cell expansion by aAPC/mOKT3 (Figure 3A). Moreover, HLA-restricted antigen-specific $CD8^+$ cytotoxic T lymphocytes (CTL) against viral and tumor antigens could be generated from $CD3^+$ T cells initially expanded for four weeks using aAPC/mOKT3 (Figure 3B and 3C). The functional avidity of these tumor antigen-specific T cells was sufficient to recognize tumor targets endogenously expressing antigen, confirming that the T cell repertoire for tumor antigen recognition was preserved (Figure 3C). We also confirmed that stimulation with aAPC/mOKT3 induced the expansion of tumor-antigen specific T cells. After 28 days in culture, MART1 peptide specific $CD8^+$ T cell expansion was 420–1,150 fold (Figure S1D).